WATER TABLE FLUCTUATIONS AND RUNOFF GENERATION IN THREE CATCHMENT TYPES IN A COASTAL TEMPERATE RAINFOREST

A Thesis

Presented to the Faculty of the Graduate School

of Cornell University

In Partial Fulfillment of the Requirements for the Degree of

Master of Science

by

Paul Anders Herendeen

August 2014

ABSTRACT

The northern Pacific perhumid coastal temperate rainforest (PCTR) extends along the Pacific coast from central British Columbia through south-central Alaska. Soil hydrology is a dominant ecosystem control in the PCTR, affecting soil formation, vegetation distribution, biogeochemical cycling, and carbon storage. Despite the importance of soil hydrology to the ecosystem, there have been few studies investigating water table dynamics and runoff generation in the PCTR. In this study, we applied two methods to investigate this interaction across a replicated set of three common sub-catchment types spanning a range of landscape units.

Over the summer and fall of 2013 we monitored sub-catchment discharge, water table position, and precipitation in order to measure catchment moisture balance and the interaction between water table and runoff. There was a strong non-linear response in the wet soil catchments (fen and forested wetland), with > 80% of runoff occurring above a threshold water table position. The hydrology of the upland sites appears to be controlled by shallow rock horizons. Despite cool summertime temperatures and frequent precipitation, catchments experience a moisture deficit during the summer months that is reflected in the water table positions and catchment runoff ratios. Because of the strong dependence of runoff on water table position, changes in seasonal moisture balance that affect the water table have the potential to cause large, non-linear changes in runoff generation and biogeochemical cycling.

We also made use of an existing five year dataset from the same catchments to model catchment storage / discharge relationships as ordinary, non-linear, first-order differential equations. Performance of the models varied across sub-catchments, simulating discharge reasonably well in some (Nash-Sutcliffe efficiency 0.20 - 0.45) and poorly in others (Nash-Sutcliffe < 0). This difference in model performance appears to be the result of un-accounted for subsurface flow. Despite the failure of the model to recreate catchment functioning across all sites, an initial comparison between modeled storage / discharge relationships and observed water table and discharge showed a correlation between modeled and physical behavior.

BIOGRAPHICAL SKETCH

Paul Herendeen was raised with a love of the outdoors, which led him to the study of ecology. After earning an undergraduate degree in Biology from the University of Virginia, he worked as a technician for the US Geological Survey Western Ecological Science Center and the US Forest Service Pacific Northwest Research Station in Juneau, AK. After years in the field, he returned to graduate school at Cornell University to study the fundamental structures of landscape ecology – water, soils, and biogeochemistry.

ACKNOWLEDGMENTS

I would first like to thank my advisors for their support in this endeavor. Dr. David D'Amore of the US Forest Service Pacific Northwest Research Station started as an excellent boss, became an exemplary advisor, and has remained a steadfast supporter. Dr. M. Todd Walter of Cornell University has allowed me to pursue my interests and has always been available to answer my questions. Dr. Jery Stedinger, also of Cornell, has never been stumped by any math question I've put to him and has made sure my logic stayed sharp. My friends and colleagues in the Soil & Water Lab have given me support both scientific and social. Field personnel from the Forest Service and Cornell University were instrumental in making this project happen, especially Mark Lukey (USFS), Dr. Adelaide Johnson (USFS), and Rosemary Yardley (Cornell). Most of all I would like to thank my wife Elizabeth, for her love and support.

TABLE OF CONTENTS

LIST OF FIGURES

LIST OF TABLES

1 Water table and runoff generation across catchment types in a perhumid coastal temperate rainforest

1.1 Introduction

The northern Pacific perhumid coastal temperate rainforest (PCTR) occupies a narrow strip along the Pacific margin of British Columbia and south-central Alaska. Water is a dominant ecosystem control in the PCTR, affecting pedogenesis (D'Amore, 2011), vegetation distribution (Neiland, 1971), biogeochemical cycling (Fellman et al., 2009), and carbon storage. Soil saturation status and water table position mediate many of these interactions, but the controls on soil water table are poorly understood.

Perhumid temperate rainforests are characterized by annual precipitation greater than 1,400mm, with > 10% falling during cool summers and transient snow in the winter (Alaback, 1996). They occur in limited areas in North and South America, Europe, and Australasia (DellaSala et al., 2011). Temperate rainforests are globally exceptional in their productivity and carbon storage (Alaback, 1991; DellaSala et al., 2011) and are important conservation targets.

Much of the PCTR within the United States lies in the 70,000 km^2 Tongass National Forest in the southeastern panhandle of Alaska. Annual precipitation in the area varies from 1500 to 5600 mm, with an average annual mean temperature of < 5°C (Nowacki et al., 2001). The region is mountainous, with widespread conifer forests (Western Hemlock (*Tsuga heterophylla*) and Sitka Spruce (*Picea sitchensis*)) along with extensive peatlands at lower elevations, transitioning to alpine tundra at higher elevations. Approximately 25% of the land area in the Tongass is wetlands (Leighty et al., 2006).

Persistent precipitation and cool temperatures promote the accumulation of dense organic carbon stocks. Carbon densities in the PCTR can exceed 300 Mg ha^{-1}, some of the highest forest carbon densities in the world (Heath et al., 2011). An estimated ~66% of this carbon stock (1.86 Pg) is belowground, with wet soils in particular estimated to have belowground carbon densities in the range of 500 – 900 Mg/ha (Leighty et al., 2006). Globally, wet soils are estimated to contain 20-30 % of the terrestrial carbon stock,

and are vulnerable to changing moisture and temperature regimes (Davidson and Janssens, 2006; Holden, 2005).

The accumulation, processing, and release of soil organic carbon stocks is strongly responsive to soil saturation (Holden, 2005). Soil respiration and dissolved CO_2 export have also been shown to respond to soil moisture status and temperature in the PCTR (D'Amore, 2011; Fellman et al., 2009). Furthermore, water table is a widely reported first-order control on production and release of methane in northern peatlands (Lai, 2009), a particular concern given methane's 100-year global warming potential of 34 times that of CO_2 (Myhre et al., 2013).

Processing and export of this soil carbon as dissolved organic carbon (DOC) is a significant source of nutrients to near-shore marine environments (Edwards et al., 2007). Annual DOC export from the three sub-catchment types considered in this study (fen, forested wetland, upland) have been estimated at 329, 306, and 77 kg ha^{-1} yr^{-1} respectively (D'Amore, 2011), among the highest values in the world (Alvarez-Cobelas et al., 2010). The quantity and chemical quality of DOC export has been shown to be affected by pathway of water flow in the soil (e.g., Hood et al., 2006; Schiff et al., 1997; Worrall et al., 2008; Zhang et al., 2007), with DOC production generally occurring in organic-rich, hydraulically conductive upper soil horizons and then flushing to streams when flowpaths through this layer are activated (Hornberger et al., 1994; Worrall et al., 2002). As such, the development shallow subsurface and overland flow in organic-rich soils is an important mechanism of watershed DOC export (McGlynn and McDonnell, 2003). Working in the same catchments as this study, Fellman et al. (2009b) showed an increase in both DOC export and lability during stormflow, with stormflow contributing a substantial percentage of total annual export. Similar results have been reported elsewhere in the region (Fitzgerald et al., 2003) and in other high-latitude peatlands (Worrall et al., 2008).

In addition to strongly affecting biogeochemical cycling, the timing and intensity of catchment discharge is critically important to Southeast Alaska's wild salmon fishery (*Oncorhynchus* spp.), valued at nearly $1 billion annually (TCW Economics, 2010). All five species of Pacific Salmon depend on

freshwater spawning habitat, and are vulnerable to changes in the timing and intensity of summertime streamflow (Bryant, 2009; Mantua et al., 2010).

Despite the importance of soil hydrology in the PCTR, there have been few studies in the area directly addressing subsurface flowpaths and runoff generating mechanisms within the soil. An early review of literature on the hydrology of Alaskan wetlands found virtually no information for southeast Alaska (Ford and Bedford, 1987), although work from several years prior was soon published describing aquifer recharge and discharge through wet soils in the region (Siegel, 1988). Many of the soil organic matter studies cited above measure and describe soil saturation, but none explicitly link water table and runoff generation.

Studies in other areas have described the importance of saturation-excess runoff generation in wetlands and peatlands: in Minnesota (Bay, 1969), the United kingdom (Daniels et al., 2008; Evans et al., 1999; Holden and Burt, 2003), Newfoundland (Price, 1992), and Ontario (Hinton et al., 1998; Taylor and Pierson, 1985). There is likewise a robust literature concerning the hydrology of steeper, forested headwater catchments in temperate rainforests, for example the many studies from the Maimai catchment in New Zealand (e.g., McGlynn et al., 2002), the HJ Andrews Experimental Forest in Oregon (e.g. Swanson and Jones, 2002), and a series of studies on forested wetlands in the Precambrian Shield of Northern Canada (Devito et al., 1996; Waddington et al., 1993). Studies in the PCTR in British Columbia showed that saturation-excess runoff generation can produce up to 95% of storm event discharge, and that more runoff is produced with shorter concentration times during wet-season events (Emili et al., 2006; Fitzgerald et al., 2003).

Given the importance of soil water table, subsurface flowpath, and runoff generation to the ecology of the PCTR, understanding the interactions between these components is critical. In this study, our aim was to investigate the interaction between soil water table and runoff generation in three common sub-catchment types in the PCTR. These sub-catchments were chosen to represent a range of common ecosystem types within the PCTR, and the interaction of water table and runoff generation has

implications for a number of landscape ecosystem functions, including carbon storage and processing, nutrient export, and streamflow dynamics.

1.2 Materials and methods

1.2.1 Site description

The study took place in the perhumid coastal temperate rainforest near Juneau, Alaska. Juneau has a temperate maritime climate, with mean annual precipitation of 1,400 mm and mean monthly temperatures ranging from -2 to 14°C. Significant rainfall occurs in all months of the year, with roughly two thirds of total precipitation falling from September through March.

The study sites were chosen to represent a range of common hydropedologic units in the PCTR. Hydropedology links hydrology, pedology, and biogeochemical processing through the movement of water, energy and material through the soil (Lin et al., 2006) and offers a natural classification of ecological types in the PCTR. The study sites consisted of three common hydropedologic units (slope fen, forested wetland, upland) replicated across three watersheds (Fish, McGinnis, and Peterson) (Figure 1.1). Fens and forested wetlands are the most commonly mapped wetland soil types in the area, and the upland sites represent a common, well-drained end-member. Hydropedologic units for the study were determined using existing soil and vegetation maps. Soil map data were confirmed in the field with soil descriptions following US Natural Resource Conservation Service standard methods (Soil Survey Division Staff, 1993). For a full description of the identification and delineation of these sub-catchments see D'Amore (2011). Site characteristics are given in Table 1.1.

The fen sub-catchments are located on footslope / toeslope landforms and had deep (>1m), moderate to well decomposed peat Histosols (Typic Cryohemist). Vegetation consists of sphagnum mosses (*Sphagnum* spp.), ericaceous shrubs, and scattered sedge (*Carex* spp.) and dwarf shore pine (*Pinus contorta* var. *contorta*). All three sites have gentle (<5%) slopes towards outlet drainages. The sites

classify as palustine emergent (National Wetland Inventory, NWI, Cowardin et al., 1979) or slope fen (National Wetlands Working Group, NWWG, National Wetlands Working Group et al., 1997).

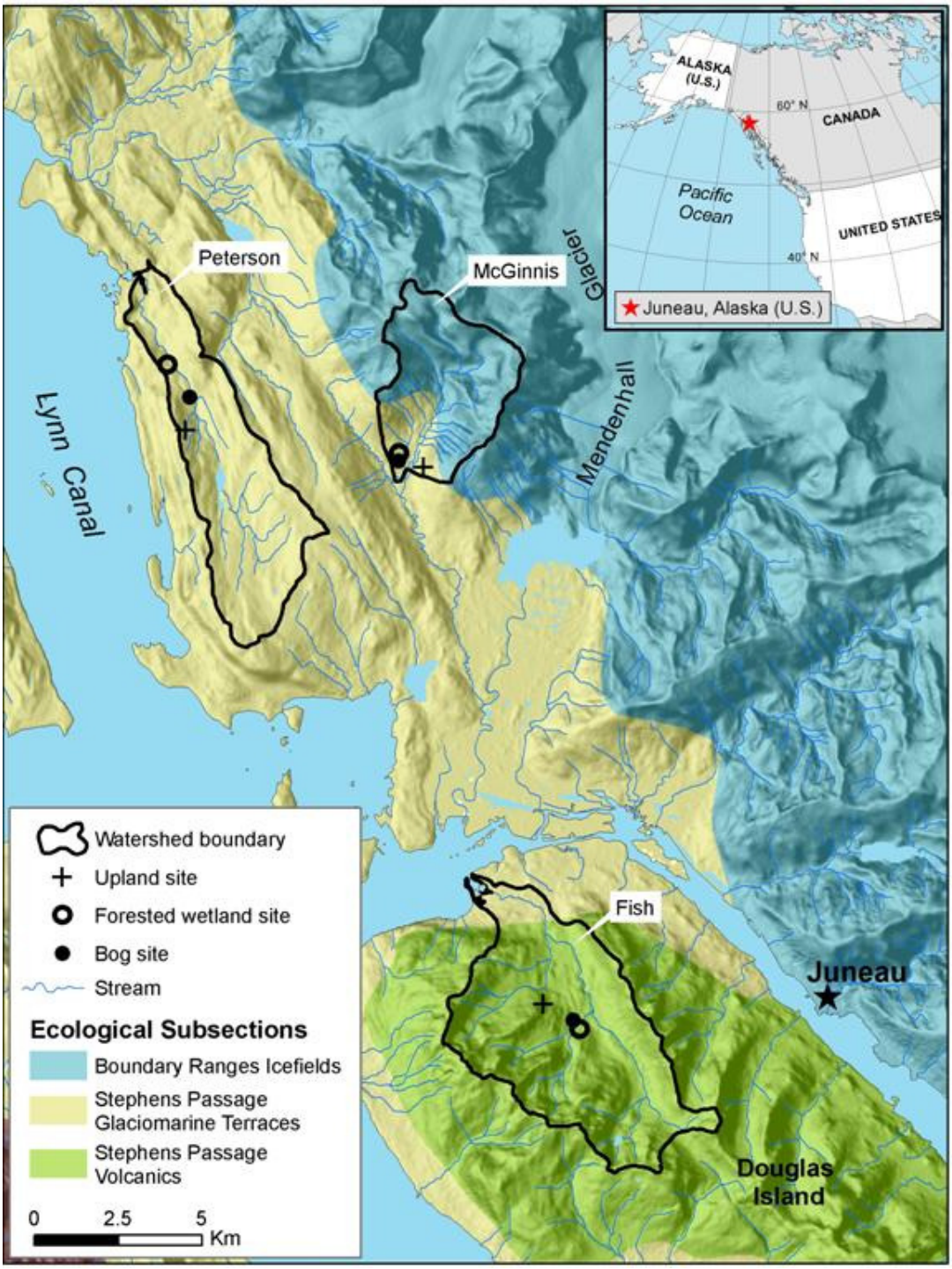

Figure 1.1. Watersheds and sub-catchments near Juneau, AK.

Table 1.1. Sub-catchment characteristics. Adapted from D'Amore (2011).

Type	Watershed	Soil subgroup	Aspect (degrees)	Elevation (m)	Slope (degrees)	Live tree BA (m^2 ha^{-1})	Live tree volume (m^3 ha^{-1})	Size (ha)
Fen								
	Fish	Typic Cryohemist	352	89	3	na	na	1.5
	McGinnis	Typic Cryohemist	123	133	3	na	na	2.1
	Peterson	Typic Cryohemist	27	112	3	na	na	1.3
Forested wetland								
	Fish	Terric Cryohemist	350	248	5	38.0	248	13.1
	McGinnis	Terric Cryohemist	94	128	19	44.5	387	4.3
	Peterson	Histic Cryaquept	55	20	5	46.6	431	2.6
Upland								
	Fish	Typic Haplocryod	343	392	15	73.5	769	2.1
	McGinnis	Typic Haplocryod	280	202	20	51.2	599	1.6
	Peterson	Lithic Haplocryod	50	163	15	60.6	657	23.7

Previous studies identified these sub-catchments as sloping bogs (NWWG). However, the input of minerotrophic groundwater is more typical of the fen type sloping wetland.

The forested wetlands have thinner peat layers (0.5 - 1m) over rock and were classified as Histosols (Terric Cryohemist) at the McGinnis and Fish sites and an Inceptisol (Typic Cryaquept) at the Peterson site. The vegetation communities consist of sphagnum moss (*Sphagnum* spp.) and a well-developed shrub understory including both obligate wetland species, such as skunk cabbage (*Lysichiton americanum*), and upland species, in particular Alaska blueberry (*Vaccenium* spp.). The overstory is a mix of Sitka Spruce and Western Hemlock. Slopes are moderately higher than in the fen sites (~5% for Peterson and Fish, ~20% for McGinnis). These sites classify as palustrine forested wetland (NWI) or bog forest (NWWG).

The upland sites are located on backslope landforms with moderately deep and moderately well-drained Spodosols (Typic or Lithic Haplocryod). These soils are thinner, with impenetrable rock layers often occurring at less than 1m depth. The vegetation community is also *Veccinnium* spp. dominated understory under Sitka Spruce / Western Hemlock, but these forests have much higher tree basal area and volume relative to the Forested Wetlands (Table 1.1). These sites represent mineral soil end-members for this study.

1.2.2 Data collection

Discharge from each sub-catchment was monitored with a Parshall flume (Plasti-Fab, Tualatin Oregon) instrumented with a recording stage logger (Solinst, Georgetown Ontario) corrected for atmospheric pressure using barometric pressure transducers at each watershed. Stage was recorded at 15 min intervals and converted to flow using manufacturer supplied stage / discharge relationships. Precipitation was measured with tipping-bucket precipitation gauges (Onset, Cape Cod Massachusetts) installed at each of the three watersheds in the fen sub-catchments. To monitor water table position in each sub-catchment, pairs of water table wells were installed adjacent to a randomly selected set of soil respiration rings previously installed for soil gas studies (D'Amore, 2011). Wells were constructed of 1.25" PVC piping with paired holes drilled at 1cm intervals and were installed to either 1m depth or the

point of refusal if less than 1m. Water level in the wells was recorded at 15 minute intervals with Solinst Leveloggers. The level recorded in the two wells was averaged to produce a single value for the sub-catchment. All instrumentation was deployed from the first week of June through the end of October, 2013.

Measured precipitation data were supplemented with data from the Juneau International Airport (PAJK), as provided by the National Climatic Data Center (http://www.ncdc.noaa.gov). Hourly data from the Global Hourly Surface Dataset were used for comparison over the time period spanned by this study, and daily and monthly normals for the period 1981-2010 (Arguez et al., 2012) were used in the calculation of average catchment moisture balance. Potential evapotranspiration (PET) was calculated using a modification of the Priestly-Taylor equation requiring only daily minimum and maximum temperatures (Archibald and Walter, 2014) and a Priestly-Taylor coefficient (α) of 1.26.

1.2.3 Data analysis

For most analyses available data were aggregated to hourly values, the exception being the single-peaked storm hydrograph analysis described in section 1.3.1. Frequent, low-intensity rainfall made identification of discrete storm events difficult. Rainfall events that produced little to no hydrograph response were of particular interest to this study, as was the total storm runoff volume for events that did produce runoff. Therefore, we defined rainfall events as beginning with the initiation of rainfall and continuing until (1) there were three consecutive hours with no precipitation and (2) the discharge flow returned to pre-event levels. Rainfall events with total precipitation amounts of less than 10 mm generally did not produce a response in water table or discharge and were excluded. Runoff volume was calculated by integrating between the response hydrograph and a constant line equal to pre-event flow. For specific analyses, rainfall events were subsampled into two overlapping groups: one for events with complete water table records for the duration of the event, and another for events that produced single peaked response hydrographs.

Discharge and water table measurements were affected by censoring. Discharge values below the measurement limits of the flumes were marked as censored and assigned a value of ½ the minimum recordable flow. For analyses sensitive to this substitution (e.g. catchment water balance) substitutions of 0 and the minimum flow were also assessed to constrain the introduced error. The water table wells were affected by both high and low censoring. Low censored values occurred when the water level dropped below the bottom of the wells; this only occurred in the upland sites. Censoring had a physical meaning in this case, as the wells were driven to the point of refusal, i.e. the impenetrable rock / till layer. Very high soil water tables sometimes exceeded the recording range of the barologgers. Because the pressure recorded by the logger is the sum of hydrostatic and barometric pressure, this censoring limit changes with barometric pressure and is not a fixed value. Two of the fen sites, Peterson and McGinnis, were heavily affected, with almost no useable water table data. The remaining fen site and the forested wetlands were minorly affected, with only scattered missing data. The uplands, because of their shallower wells, were unaffected.

1.3 Results

1.3.1 Catchment Hydrology

Precipitation at the Fish, Peterson, and Juneau Airport sites was highly similar, with ~825 mm of rainfall over the period of the study, representing roughly half of the average annual precipitation (Figure 1.2). The McGinnis site received substantially more precipitation (~1000 mm total). This variation in precipitation across short distances is characteristic of the area; annual precipitation totals can vary by 50% across less than 20km (NOAA 1981-2010 annual normals, cf. Arguez et al., 2012). Precipitation at the Juneau Airport was 8% higher than the 1981-2010 average over the period of the study. The relative frequency of rainfall intensities in shown in Figure 1.3, highlighting the preponderance of low-intensity rainfall.

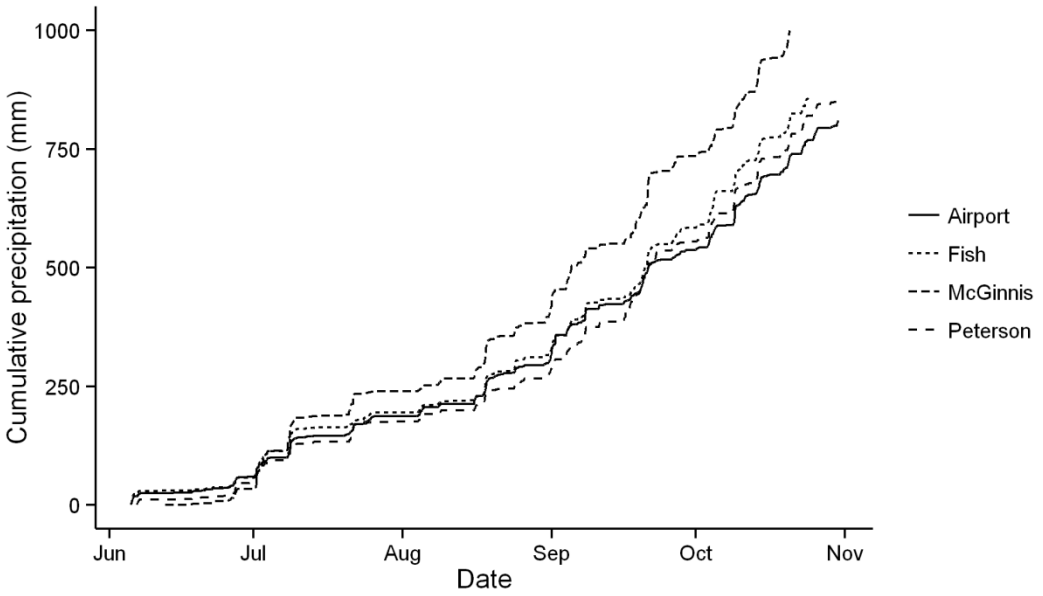

Figure 1.2. Cumulative precipitation for the three study watersheds and the Juneau Airport.

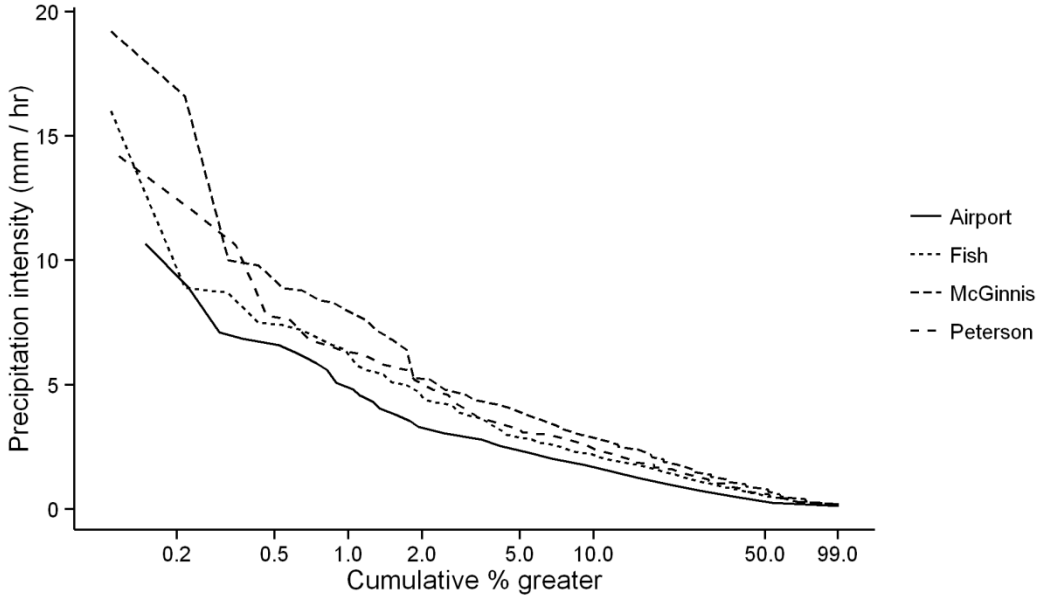

Figure 1.3. Hourly precipitation intensity.

Discharge at all study sites showed pronounced flashiness and frequent periods of very low flow (Figure 1.4). In particular, the upland sites show extensive periods of low-censored flow, even during periods of rainfall. Although infrequent, high flows contribute a significant portion of total runoff. The percentage of total runoff contributed by storms with a probability of exceedance of < 25% during the period of the study was 74-78% for the fens, 80-83% for the forested wetlands, and 64-83% for the uplands.

The tendency for runoff-producing events to occur as part of complex rainfall events and the resulting difficulty in identifying discrete storm peaks resulted in a small number of storms producing single-peaked hydrographs amenable to traditional hydrograph analysis (Table 1.2). Because precipitation in the PCTR tends to be persistent and low intensity, and because the centroid calculation is sensitive to even small values far along the axis of integration, an adjusted precipitation centroid was defined by excluding precipitation falling after both the hydrograph peak and three hours with no more than 0.2 mm total precipitation.

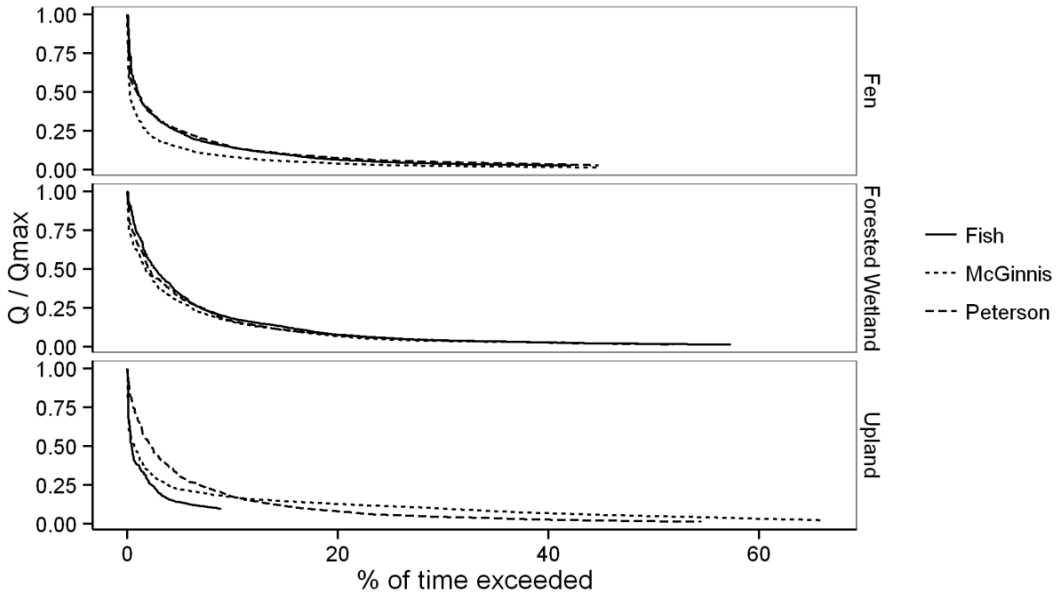

Figure 1.4. Flow frequency plots for the study sub-catchments. Flows have been scaled relative to their maximum values. Curves do not extend to 100% due to data censoring at low values of discharge.

Table 1.2. Statistics for single-peaked storm hydrographs. Lag is the time in hours from the centroid of precipitation to the centroid of the discharge hydrograph. The adjusted lag uses the adjusted precipitation centroid described in section 1.3.1

Type	Watershed	centroid to centroid lag (st. dev.) (hours)	adjusted centroid to centroid lag (st. dev.) (hours)	# of storms
Fen				
	Fish	6.4 (1.7)	3.8 (2.3)	4
	McGinnis	4.4 (1.4)	4.6 (4)	10
	Peterson	8.5 (1.7)	7.9 (4.1)	7
Forested Wetland				
	Fish	8.7 (1.3)	4.6 (2.6)	5
	McGinnis	5.6 (1.4)	3.9 (1.6)	6
	Peterson	10.3 (3)	7.1 (2.5)	5
Upland				
	Fish	10.4 (2.4)	7.7 (4.5)	4
	McGinnis	8.1 (1.9)	5.9 (4)	7
	Peterson	11 (1.8)	6.5 (2.4)	4

Figure 1.5 shows the monthly water balance for the period of this study, along with the 1981-2010 normals as calculated at the Juneau Airport site. A pronounced seasonal pattern is apparent, with a negative to slightly positive moisture balance during the months of April through August. A substantial increase in precipitation and decrease in PET in September produces a large moisture excess, with the increase in precipitation contributing approximately 2/3rds of the change to a positive moisture balance. For the remaining fall and winter months, PET approaches zero and the moisture balance essentially equals the precipitation input. The calculated normal annual precipitation and PET at the airport were 1580 mm and 640 mm, respectively.

The moisture balance shown is based on measured precipitation and theoretical PET, three additional factors should be considered in estimating actual catchment moisture balance. First, in most years a significant winter snowpack accumulates and releases water in the spring, often through the month of May, adding to the precipitation input and potentially changing the moisture balance to positive. Second, evapotranspiration may not reach the potential rate. In particular, the fens and forested wetlands have

poor hydrologic conductance through the *Sphagnum* surface layer, and a lack of widespread vascular plants. Working a Newfoundland bog Price (1992) reported mean values of the Priestly-Taylor coefficient α of 0.87 to 0.99 depending on weather. Finally, subsurface flow into and out of the sub-catchments may alter the moisture balance.

The calculated change in water balance is quite large between the summer and fall months and is reflected in catchment runoff ratios (Figure 1.6). All sub-catchments show a pronounced decline in runoff ratio during the summer months, with values 25-75% of their fall maxima. There is also a pronounced seasonal difference in water table position (section 1.3.2). Taken together, these results show a clear period of negative or near-negative water balance being driven largely by precipitation input.

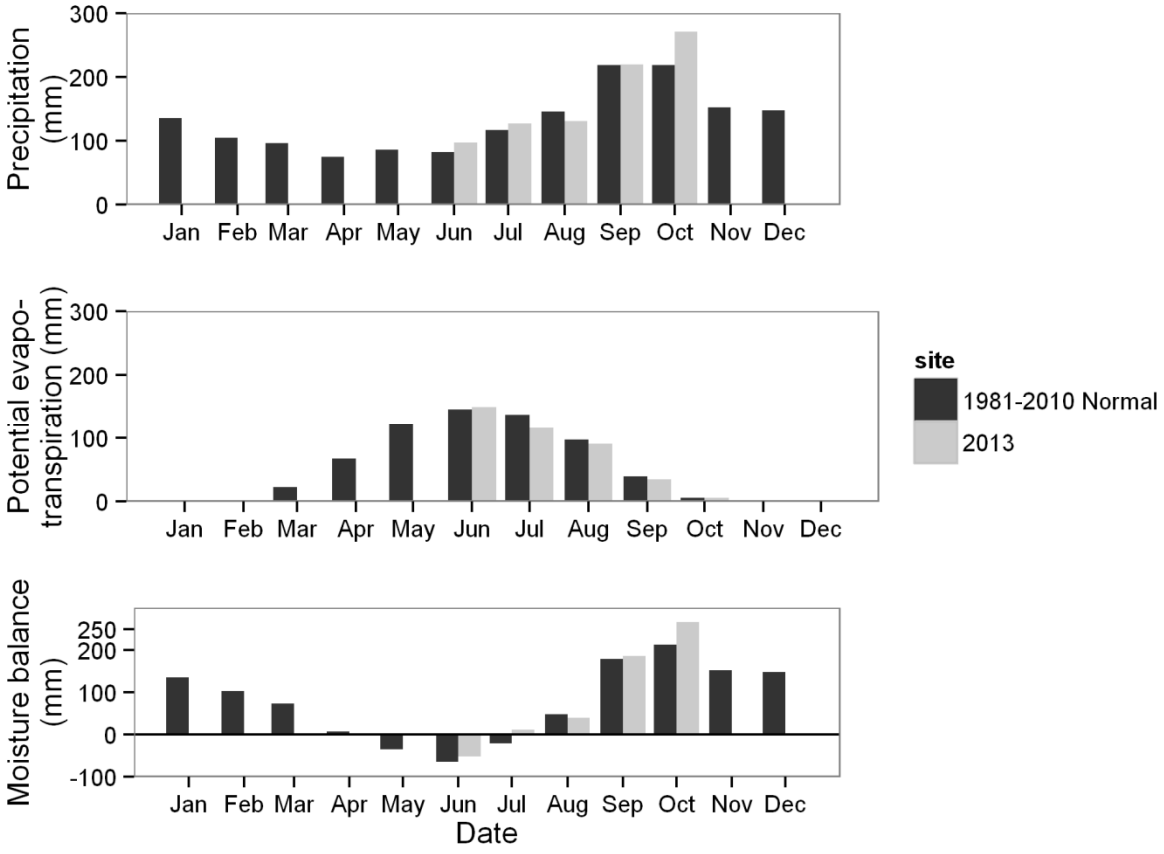

Figure 1.5. Moisture balance at the Juneau Airport.

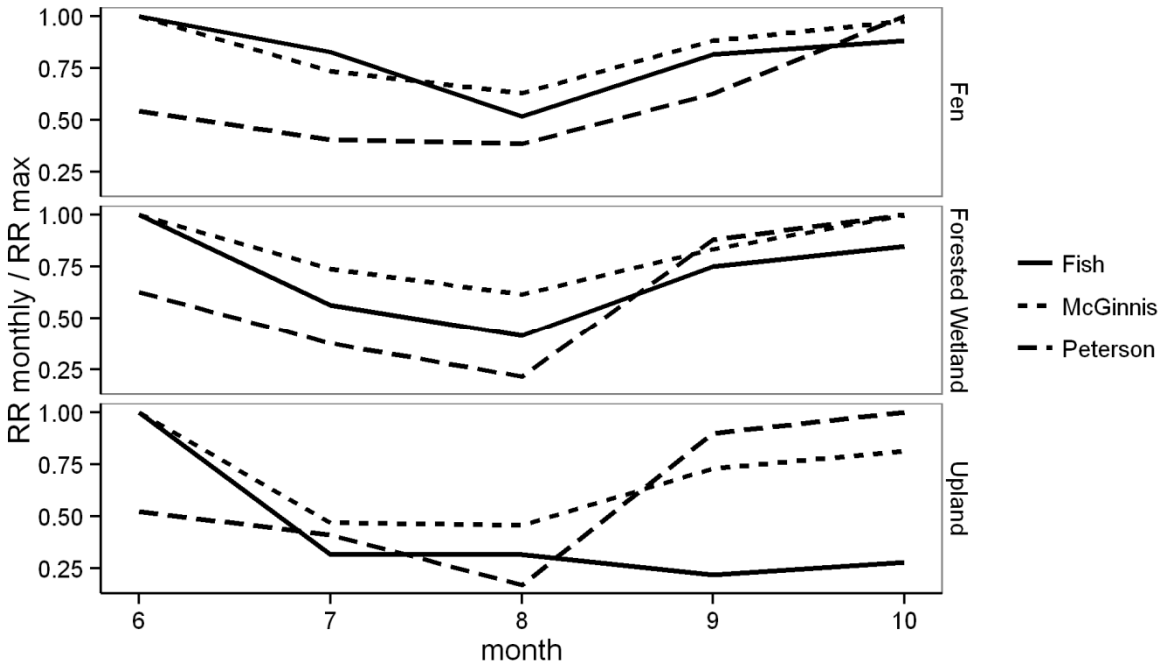

Figure 1.6. Scaled runoff ratios for sub-catchments. Monthly values have been divided by the maximum monthly value for each sub-catchment.

1.3.2 Water table and runoff dynamics

Water table position in all sub-catchments shows a distinct seasonality, with the summer months (June-July-August) exhibiting lower average water table position compared to the fall (September-October) (Figure 1.7). This relationship is readily apparent in water table residence time plots (Figure 1.8). Notable in both figures is the significantly higher water table in the Peterson upland, relative to the other two uplands.

Water table position is closely linked with discharge. The fens and forested wetlands and, to a lesser extent, uplands all show a strong non-linear relationship between water table position and runoff (Figure 1.9). Very little runoff occurs at lower water table positions, and above a threshold there is a wide range of discharge values across a narrow band of water table positions.

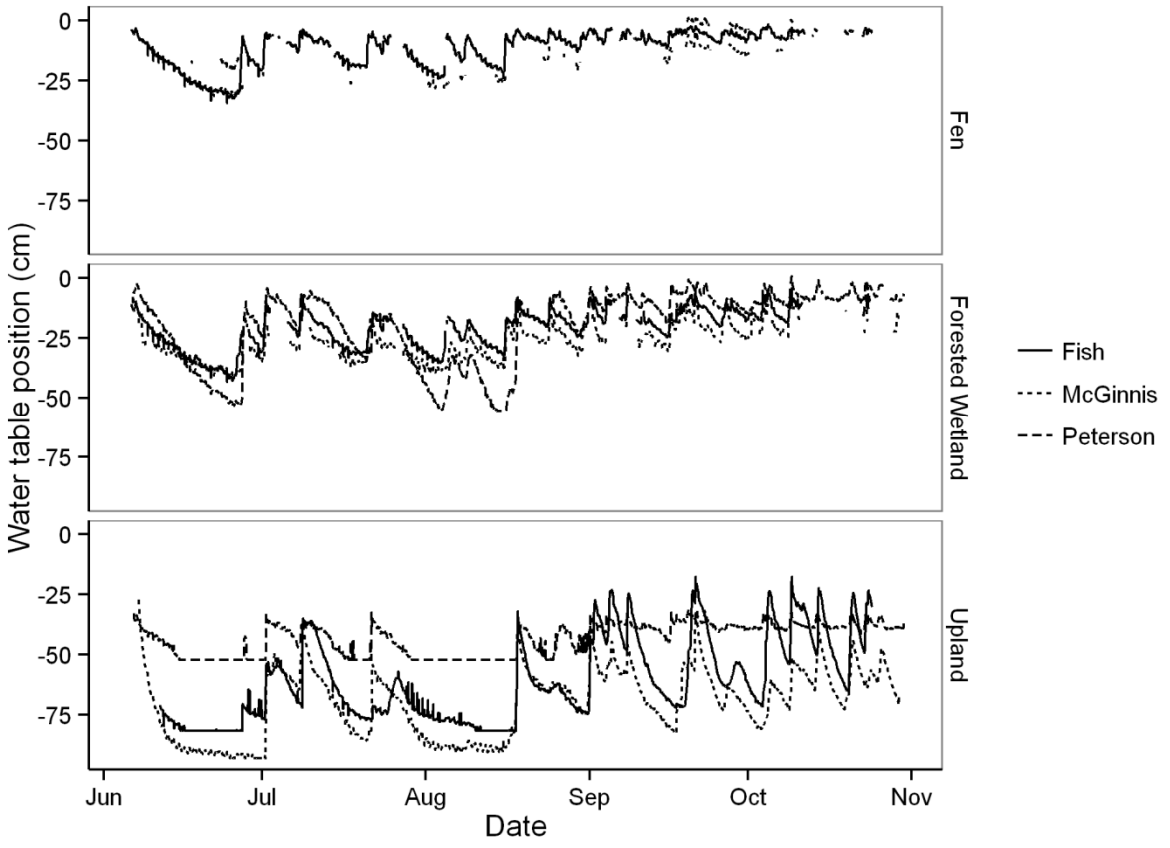

Figure 1.7. Water table position for sub-catchments. 0 is the soil surface. Constant horizontal lines in the upland record indicate periods of dry wells.

The precise location of the soil storage / discharge threshold is difficult to determine for several reasons: (1) while the effect is strongly non-linear, it is not binary, and rather occurs over a narrow range of water table positions, (2) there is considerable heterogeneity in soil structure in this complex terrain, so assigning a single threshold value for an entire sub-catchment may be misleading. Nevertheless, it is possible to determine the approximate locations of the thresholds as observed and to compare these with nearby soil profiles. We determined soil threshold locations by visual inspection of water table / discharge plots (Figure 1.9; Table 1.3). The fens produced discharge in the upper 10cm of the profile. In the forested wetlands, discharge initiates around between -10 to -21 cm and increases rapidly over a window of around 10cm to the maximum water table height.

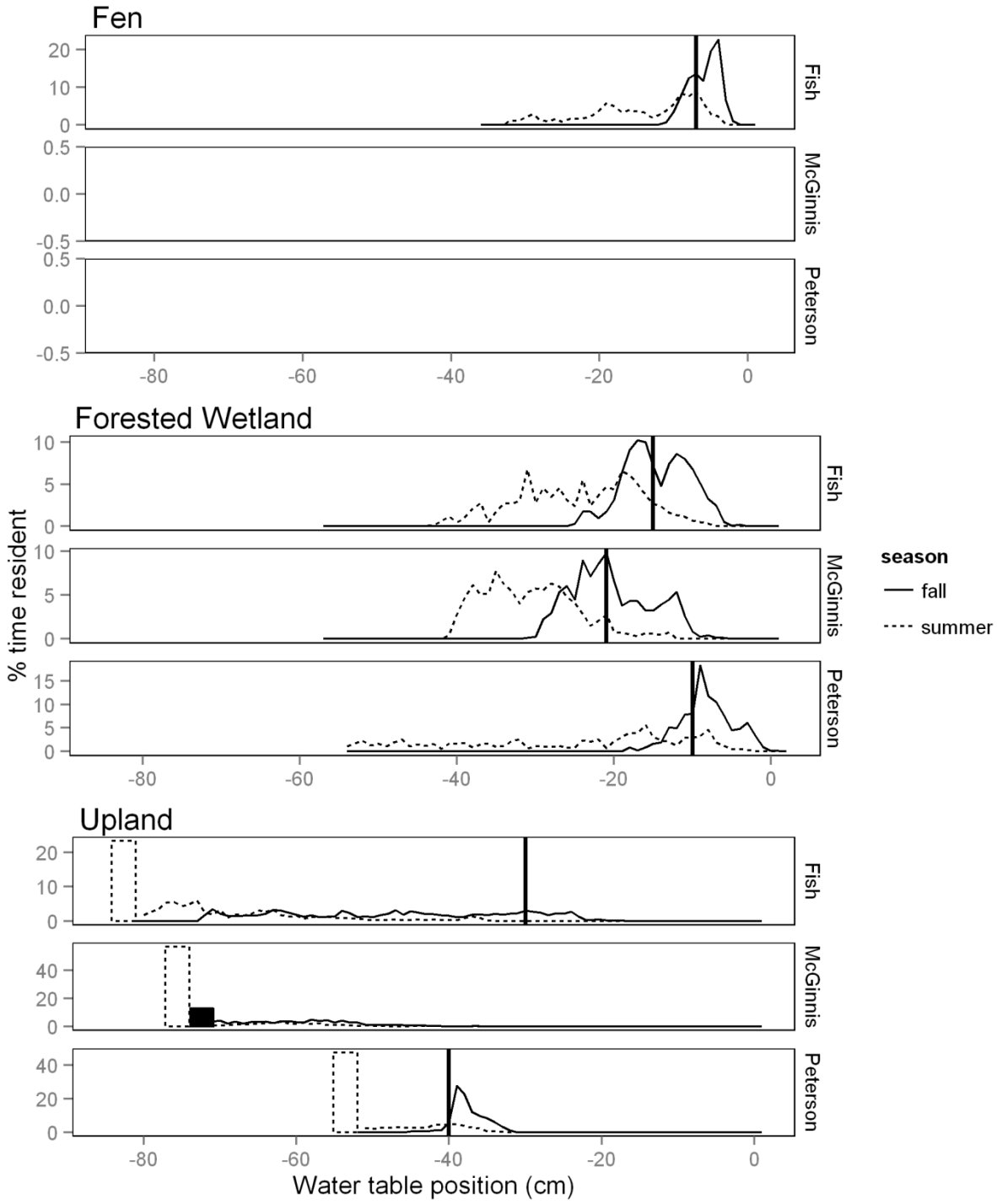

Figure 1.8. Residence times for water table position. Summer is June-July-August, fall is September-October. Vertical lines show water table thresholds as defined in section 1.3.2. Bars represent dry wells. Note that y-axis varies between panels. Data gaps prevented calculation of residence time for the Peterson and McGinnis fens.

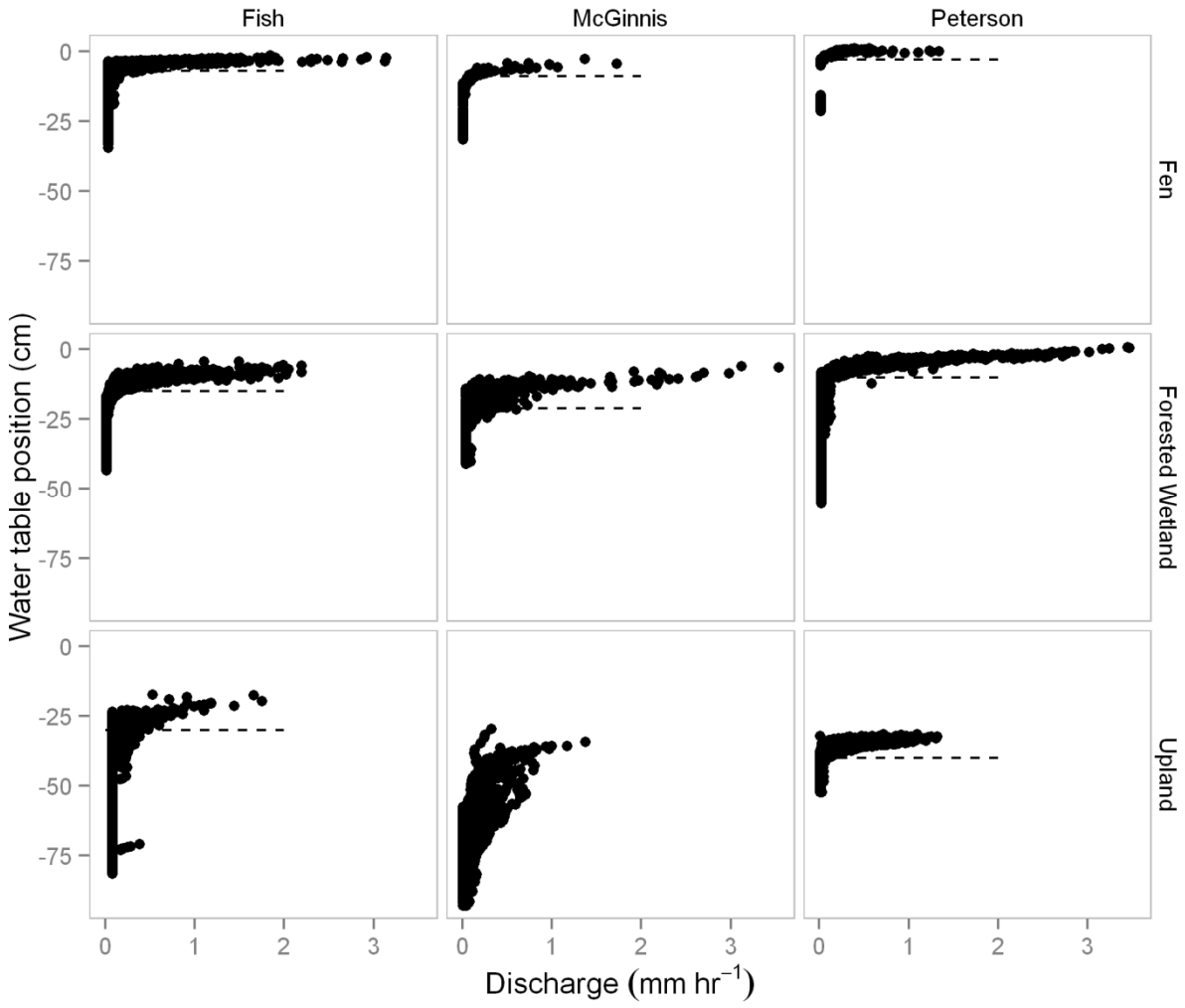

Figure 1.9. Water table / runoff relationships. Dashed lines show threshold water table positions as described in section 1.3.2.

In the fen and forested wetland sites with complete water table records, 80 – 90 % of total discharge was produced when the water table was above the threshold value.

The upland sites show more variation water table / runoff relationships. The McGinnis upland produces discharge across a wide range of water table positions, while the Peterson upland shows a threshold response similar to the fens and forested wetlands, although it occurs deeper in the soil profile.

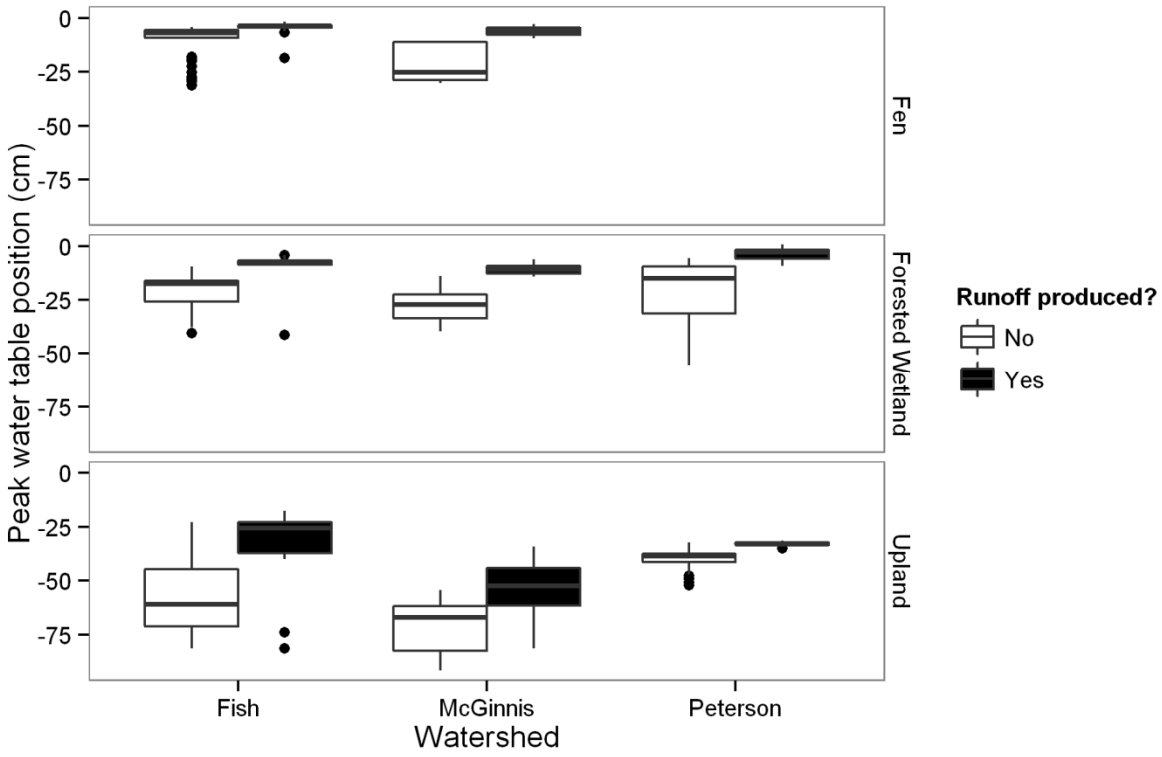

Figure 1.10. Maximum water table position during rainfall events that did and did not produce runoff (defined as runoff ratio > 0.05). Insufficient data were available for the Peterson fen site.

Table 1.3. Water table summary statistics by season for sub-catchments.

Site	Water table position (cm) minimum	threshold	mean summer (st. dev.)	mean fall (st. dev.)	% discharge above threshold
Fen					
Fish	-35	-7	-14 (7)	-6 (2)	80
McGinnis	-32	-9	-26[a] (4)	-11[a] (3)	58[a]
Peterson	-21	-3	-18[a] (1)	-2[a] (2)	95[a]
Forested Wetland					
Fish	-43	-15	-25 (8)	-15 (4)	83
McGinnis	-41	-21	-31 (6)	-20[a] (5)	68[a]
Peterson	-56	-10	-27 (15)	-8 (3)	90
Upland					
Fish	< -82	-30	-70 (17)	-47 (15)	21[b]
McGinnis	< -93	NA	-76 (14)	-62 (10)	NA[b]
Peterson	< -52	-38	-47 (7)	-38 (2)	81[b]

[a] These values are affected by missing water table position data (see section 2.5).
[b] These values are sensitive to the value of discharge applied to low-censored flows

This matches the pattern seen in the water table position plots (Figure 1.7), potentially due a less permeable bedrock layer at the base of the soil profile.

Plotting maximum water table height for storms (Figure 1.10) shows that in the fens and forested wetlands storms that do not raise the water table to the threshold fail to produce runoff, and also that once runoff is activated the further rise in the water table is limited to a narrow range. This suggests a pattern where precipitation inputs bring up the water table but do not produce runoff until the threshold is reached, after which the bulk of precipitation is routed to discharge.

In this case, the production of runoff from rainfall events will depend on both the antecedent water table position and total precipitation received. Figure 1.11 plots storm runoff ratio against antecedent water table position for storms of varying sizes. With low antecedent water table position, smaller storms produce very little runoff but larger storms are still able to convert a significant proportion of precipitation to runoff. At higher water table positions small storms are able to produce higher runoff ratios.

The influence of antecedent water table and total precipitation on runoff ratio was tested with a linear mixed-model approach using the package nlme (Pinheiro et al. 2014) in R (R Core Team, 2014). Antecedent water table and total storm precipitation were included as fixed effects with an interaction between them, and watershed was included as a random intercept effect. Each sub-catchment type was modeled separately. Because of the lack of water table data at the Peterson and McGinnis fens, only the Fish fen was used in the analysis. Antecedent water table and total precipitation were both standardized by subtracting their mean and dividing by their standard deviation. Collinearity between antecedent water table and total precipitation was assessed with the variance inflation factor (VIF).

In all sub-catchments runoff ratio was significantly predicted by both total precipitation and antecedent water table ($p < 0.01$; Table 1.4). The fixed effects represent the slope between the normalized predictor variable and the normalized runoff ratio. The magnitude of the effect of the antecedent water table was larger than that of precipitation by 27%, 108%, and 33% in the fen, forested wetlands, and uplands, respectively. The effect of the antecedent / precipitation interaction was non-significant in all

sub-catchment types ($p > 0.05$), although it did approach that significance level in the forested wetlands ($p = 0.07$) with a magnitude roughly 2/3 that of the precipitation effect and 1/3 that of the antecedent water table effect.

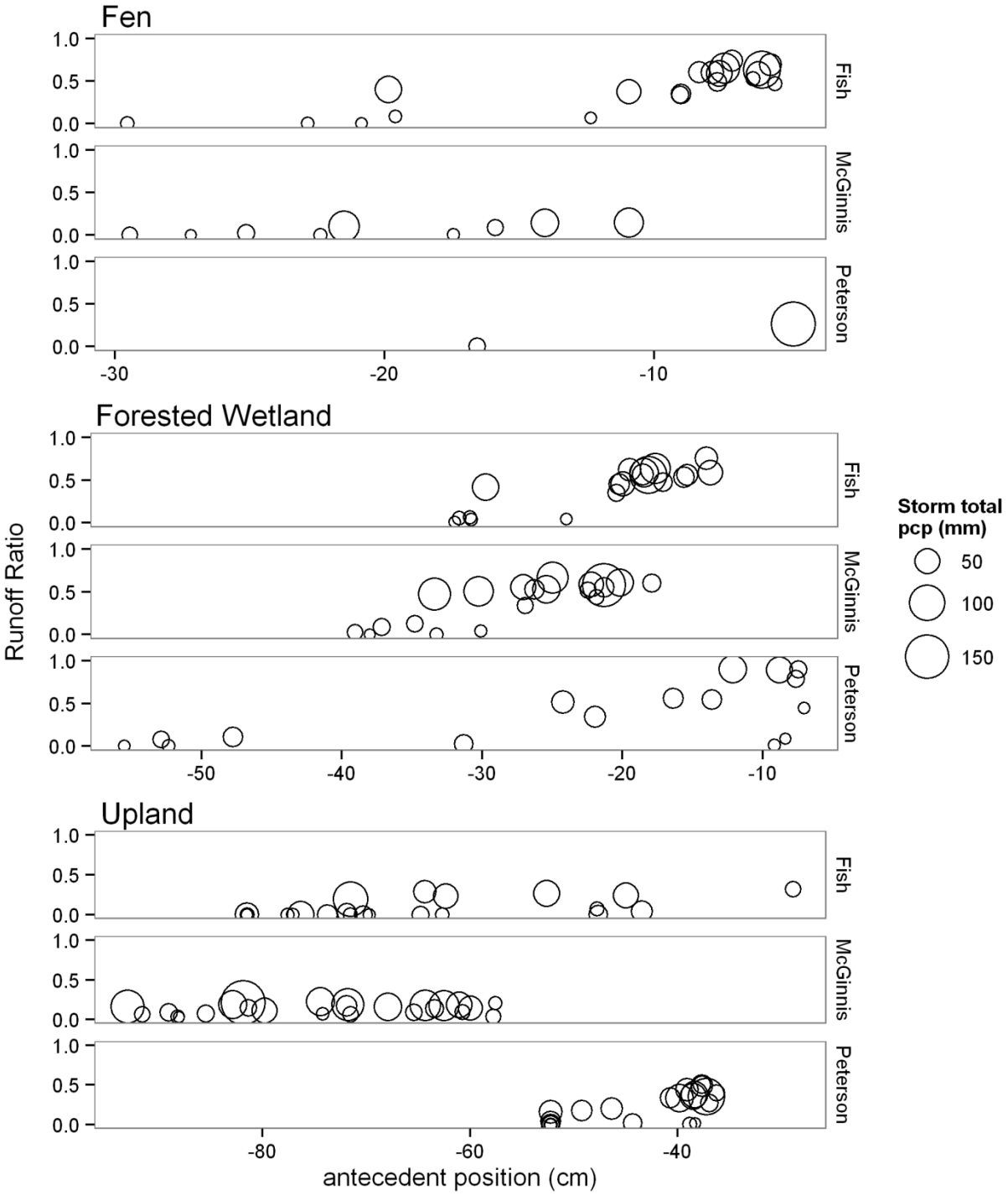

Figure 1.11. Storm runoff ratio versus antecedent water table position.

Table 1.4. Results of statistical modeling of the effect of antecedent water table (ant) and total precipitation (pcp) on runoff ratio (rr). The model is rr ~ ant + pcp + ant:pcp, random = ~ 1 | watershed, fit by REML using the package nlme in R. VIF is the variance inflation factor. # obs and # groups are the number of observations and groups, respectively.

	Fixed effects						Random effects				VIF		
		estimate	std. error	df	t-value	p-value		StdDev	# obs	# groups	ant	pcp	ant:pcp
Fen	Intercept	0.43	0.075	16	5.75	<0.0001	Intercept	0.069	20	1	1.5	1.9	1.7
	pcp	0.11	0.033	16	3.22	0.0054	Residual	0.116					
	ant	0.14	0.037	16	3.86	0.0014							
	pcp:ant	-0.05	0.038	16	-1.42	0.1738							
Forested wetland	Intercept	0.43	0.045	53	9.67	<0.0001	Intercept	0.061	59	3	1.2	2.0	1.9
	pcp	0.12	0.028	53	4.38	0.0001	Residual	0.196					
	ant	0.25	0.037	53	6.62	<0.0001							
	pcp:ant	0.09	0.049	53	1.82	0.0741							
Upland	Intercept	0.14	0.023	62	6.01	<0.0001	Intercept	0.034	68	3	1.2	1.0	1.2
	pcp	0.06	0.013	62	4.77	<0.0001	Residual	0.100					
	ant	0.08	0.016	62	4.94	<0.0001							
	pcp:ant	0.02	0.012	62	1.42	0.1601							

Note that in this case the lack of a significant interaction term does not mean there is no physical interaction of the two predictors; rather it shows a lack of a significant *change* in the interaction between them across their ranges. Both total precipitation and antecedent water table are highly significant predictors of runoff ratio and should be included in modeling runoff generation.

1.3.3 Comparison with observed morphology

Soil profile descriptions for the sub-catchment sites were performed during the initial survey of the sites and published in D'Amore (2011). All fen sub-catchments had O horizons consisting of peat in various stages of decomposition to the depth of the control section. The Fish and McGinnis fens had a fibric upper horizon, with a transition to hemic and a decrease in fiber content at around 13 cm depth for both sites. The Peterson fen had no fibric horizon, and instead had a hemic surface horizon with no clear decline in fiber content in the upper soil profile. The remainder of all three profiles was hemic. The threshold water table position in these sites occurred roughly around the location of the fibric / hemic transition, where present.

The forested wetland sites also had surface O horizons, extending to 26 – 70cm depth. Two of the sites, Peterson and McGinnis, had sapric layers in the upper profile, Peterson from 0-26 cm and McGinnis from 4-23 cm. Beneath the organic horizons was generally a B horizon of several decimeters followed by rock (C horizon). The water table / discharge threshold in the McGinnis forested wetland roughly corresponded to the transition from sapric (above) to hemic (below) and roughly at a decline in fiber content in the Peterson and Fish sites.

The upland sites showed more soil development, with a surface O horizon of 10-20cm followed by a ~10cm zone of eluviation (E) and several decimeters of illuvial horizons (Bh, Bs), the characteristic pattern of spodosols. All three upland profiles terminated in rock layers (C) at less than 1m depth. Where a threshold was present (Peterson, Fish), it occurred within the ~25cm thick Bs horizon. One upland sub-catchment (Fish) showed a discharge peak when the water table was at rock interface (upper C horizon).

The development of spodosols on the upland sites requires significant downward flux through the upper parts of the horizon and downward and /or lateral flux through the deeper layers. In contrast, the development of peat in the fens and forested wetlands suggests a persistent saturated state, with any drainage through the deep profile slow enough to maintain a high water table.

1.3.4 Controls on water table

To investigate the rate of water table drawdown, we calculated the rate of elevation decline over non-overlapping 6 hour periods with no rainfall (Figure 1.12). Drawdown rate was modeled as an effect of two categorical variables: threshold (above / below) and season (summer / fall), with watershed as a random intercept term. Each sub-catchment type was modeled separately. Because of the lack of water table data at the Peterson and McGinnis fens, only the Fish fen was modeled.

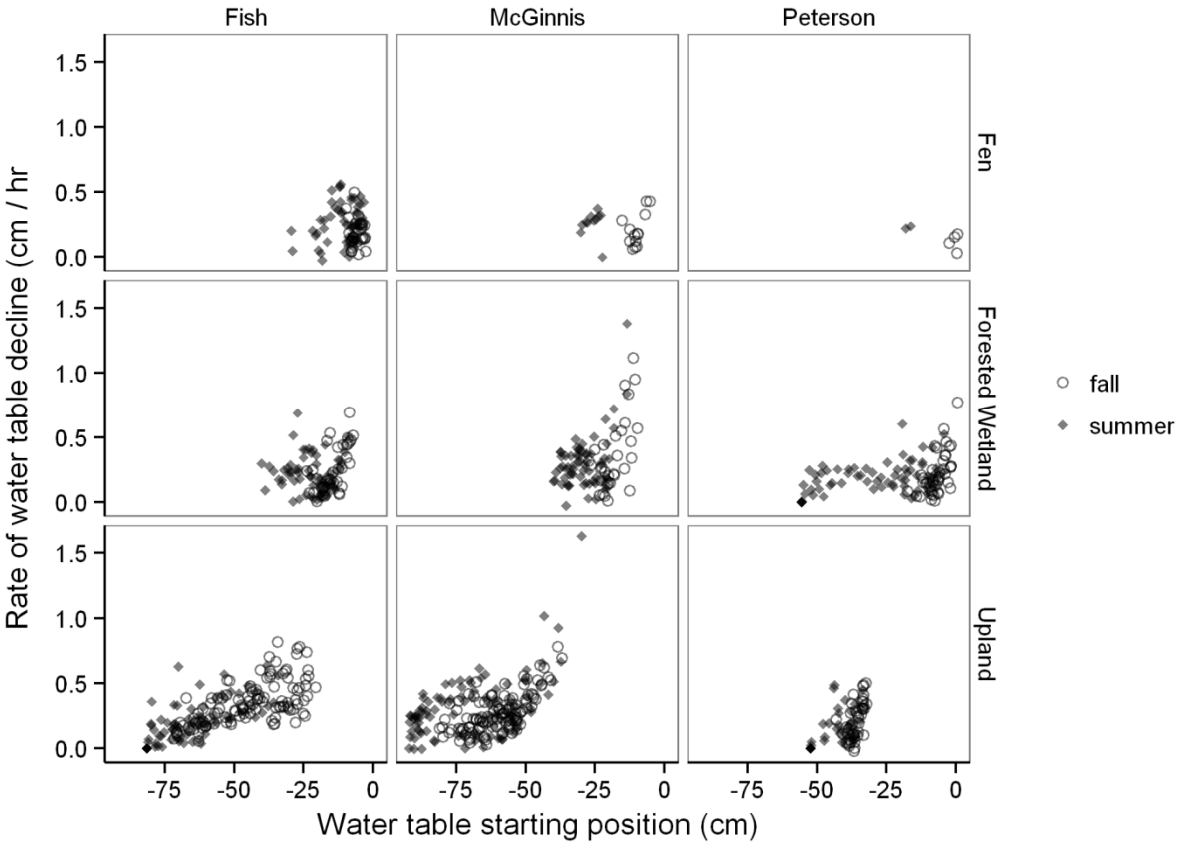

Figure 1.12. Rate of water table decline during droughts versus water table starting position.

Table 1.5. Results from statistical modeling of water table drawdown rate above and below the discharge threshold (abvthold) and between the summer and fall (summer), with watershed as a random intercept effect. Rate is in mm hr^{-1}.
The model is: rate ~ abvthold + season , random = ~1 | watershed, fit by REML using the package nlme in R.

		Fixed effects					Random effects				VIF
		estimate	std. error	df	t-value	p-value		StdDev	# obs	# groups	pcp
Fen	Intercept	1.631	0.535	81	3.05	0.0031	Intercept	0.069	20	1	1.20
	abvthold	0.386	0.330	81	1.17	0.2458	Residual	0.116			
	summer	0.810	0.348	81	2.33	0.0224					
Forested wetland	Intercept	1.776	0.443	308	4.01	0.0001	Intercept	0.061	59	3	1.4
	abvthold	1.382	0.239	308	5.78	<0.0001	Residual	0.196			
	summer	0.393	0.233	308	1.69	0.0929					
Upland	Intercept	2.584	0.568	309	4.55	<0.0001	Intercept	0.034	68	3	1.2
	abvthold	0.713	0.292	309	2.44	0.0153	Residual	0.100			
	summer	-1.537	0.200	309	-7.69	<0.0001					

Collinearity between the predictors was assessed with the variance inflation factor. Models including a threshold / season interaction were also fit, but were rejected due to relatively higher AIC (Akaike Information Criterion) and non-significance of the interaction term. The base rate of decline was 1.6, 1.8, and 2.6 mm hr^{1} for the fens, forested wetlands, and uplands, respectively (Table 1.5). There was a significant increase in drawdown rate above the discharge threshold in the forested wetlands (1.4 mm hr^{-1}, $p < 0.0001$) and uplands (0.7 mm hr^{-1}, $p = 0.015$), but the effect in the fens was non-significant (0.4 mm hr^{-1}, $p = 0.25$). Drawdown rates in the summer were significantly higher in the fen (0.8 mm hr^{-1}, $p = 0.022$), higher in the forested wetlands, although only significant at the 10% level (0.4 mm hr^{-1}, $p = 0.093$), and significantly lower in the uplands (-1.5 mm hr^{-1}, $p < 0.001$).

Water table rise during rainfall and below the discharge threshold was rapid, with mean rates of 10, 9.0, and 9.5 mm hr^{-1} for the fen, forested wetland, and upland sites. The rate of rise was strongly correlated with the rate of precipitation ($p < 0.01$ for all sub-catchment types). For storms that produced discharge (runoff ratio > 0.05), the rate of water table rise from the time the threshold is reached to the end of precipitation was -1.0, -2.0, and -0.9 mm hr^{-1} for the fen, forested wetland, and upland sub-catchments. This shows that once discharge is initiated further rise in the water table is limited even as precipitation continues to fall.

1.4 Discussion

Discharge in the fen and forested wetland sites displays a clear threshold response to changes in water table position. Infiltration and water table rise during rainfall is rapid and little runoff is produced while the water table is below the threshold position. Once the water table rises above this threshold, runoff is rapid and further rise in the water table is limited. The water table rarely reached the soil surface; rather this region of rapid discharge was in the upper 10cm (fens) or between 10-20 cm depth (forested wetlands). Previous studies in blanket peats have shown similar water table / discharge threshold responses, with nearly the entirety of discharge produced when the water table was within 5-15 cm of the peat surface (Emili and Price, 2006; Holden and Burt, 2003). Analogous patterns have also been observed

in the northeastern United States (Dahlke et al., 2012; Lyon et al., 2006). Notably, the forested wetlands do not produce overland flow, but rather very rapid sub-surface flow at around 10 – 20cm depth, indicating the presence hydrological flowpaths in this part of the profile that are activated by saturation.

Despite the persistent summer rainfall and cool temperatures, there is a period of negative moisture balance during the summer in the PCTR. This moisture deficit creates seasonal differences in water table position. Water table exerts a strong control on runoff generation, so changes in catchment moisture balance have the potential to strongly affect runoff generation and biogeochemical flushing. As the climate in the PCTR changes, the balance between precipitation and evapotranspiration may produce non-linear changes in streamflow and soil organic matter mobilization. For example, over the coming decades the PCTR is projected to become both warmer and wetter (Scenarios Network for Alaska and Arctic Planning, 2014). A shift from snowfall to rain during the winter could reduce meltwater inputs in the early spring, lowering the moisture balance and strongly impacting early season runoff. Summertime increases in temperature will most likely increase rates of soil organic matter mobilization and gas exchange, but dissolved fluxes will depend on the balance between increased PET and precipitation as it affects the water table position and hence runoff generation and soil flushing. Likewise, maintenance of summertime flow and timing of salmon spawning runs may respond non-linearly to this PET / precipitation balance.

The strong threshold response in the peatland sites naturally suggests division of the soil profile into two functional layers. The acrotelm / catotelm division has long been incorporated into peat hydrology, beginning in Russia in the mid-twentieth century and introduced to the west by Ingram (1978) and Clymo (1984) (see Holden and Burt (2003) for a review). In the original conception, peat soils were separated into a permanently saturated, low conductivity, slow-decomposition lower layer (catotelm) and an intermittently saturated high conductivity, fast decomposition upper layer (actotelm). The longevity of this classification speaks to its utility, but it fails to completely capture biogeochemical processes in peat, and a number of revisions have been proposed (Morris et al., 2011). The observed water table / discharge threshold in the PCTR occurs several decimeters above the maximum water table depth, placing it well

within the classical acrotelm. Rather, we suggest following Morris et al. (2011) and refering to the two zones as hydrologically fast and hydrologically slow.

Water table / discharge plots in the uplands show a similar, although less pronounced, threshold response. However, the interaction between antecedent water table and runoff ratio is not as apparent at these sites. All upland sites are underlain by low-permeability rock layers at < 1m depth, with saturated hydraulic conductivity several orders of magnitude lower than in the soil profile. The observed patterns of water table / discharge and antecedent water table / runoff ratio could be produced by ponding of water in the soil profile following rainfall, followed by lateral and, to a lesser extent, vertical draining. The Peterson upland is underlain by bedrock and exhibits the shallowest and most tightly constrained of the upland soil water tables. In contrast, the McGinnis upland has more permeable rock and shows the deepest water table, with wells driven to the till interface frequently dry throughout the study. The Fish watershed exhibits water table behavior somewhat between the other two sites: the water table drops below the rock interface during the summer, but is maintained above it during the fall. Tromp-van Meerveld and McDonnell (2006) and Graham and McDonnell (2010) described a bedrock-mediated “fill and spill” mechanism in the Panola and Maimai catchments ; it is possible a similar mechanism is at work here.

A clear soil-morphological correlate to the discharge threshold was not observed in the fens and forested wetlands. Discharge in the fens was roughly associated with the upper, fibric soil horizon, potentially because of the higher fiber content and greater hydraulic conductivity. The fen at Peterson, with no fibric upper horizon, also had the highest discharge threshold, with the majority of discharge happening within several centimeters of the peat surface. The causality of the morphology / hydrology relationship is not clear; the lower, more decomposed layers may restrict water flow, while the saturated state restricts root penetration and decomposition, leading to an accumulation of dense organic matter.

In the forested wetlands, the discharge threshold occurred within the O horizon. Two sites (Peterson and Fish) showed a weak increase in fiber content above the threshold, while the third (McGinnis), showed a marked decrease in fiber content and transition from sapric (above) to fibric (below).

Discharge thresholds in the uplands, where they occur, are located within the lower Bs horizons. No ponding was observed at these horizons, so while the permeability may be low enough to restrict lateral, down-slope flow they were able to accommodate vertical infiltration at rates equal to inputs from higher in the profile.

1.5 Conclusions

Wet soils in the PCTR show a clear threshold response of runoff to water table position. There is a critical depth in the soil profile, < 10cm for the fens and 10 – 20 cm for the forested wetlands, below which very little (< 20%) runoff occurs. Rainfall events that fail to bring the water table up to this elevation produce very little runoff. Once this threshold is reached the majority of precipitation is directed to outflow and further water table rise is limited. The hydrology of the upland sites appears to be controlled by the underlying rock horizons. Despite the cool temperatures and abundant summertime precipitation, catchments in the PCTR experience a moisture deficit during the summer months, with a corresponding drop in water tables and runoff ratios. The balance between precipitation and evapotranspiration has a strong effect on the water table, which in turn controls runoff. Therefore, changes in the catchment moisture balance have the potential to produce non-linear effects in runoff generation and biogeochemical fluxes from these systems.

2 Catchment classification using dynamical modeling in a perhumid coastal temperate rainforest

2.1 Introduction

The last several decades have seen considerable progress in describing the heterogeneity of runoff generating processes in watersheds. Highly detailed hydrological models are able to accurately reproduce runoff patterns, but often at the cost of extensive input data requirements, a high degree of operator skill, and the potential for over-parameterization (Beven, 2006, 2001). Understanding of runoff generation processes at the hillslope scale has been difficult to extend to the watershed scale (Troch et al., 2009), particularly when applied to ungauged basins (Hrachowitz et al., 2013; Sivapalan, 2003). Moving towards an underlying theory of watershed hydrology is widely seen as critical to the advancement of hydrological science (Dooge, 1986; McDonnell et al., 2007), especially as we struggle to manage water resources in a changing climate (Wagener et al., 2010).

Many of the challenges in developing catchment-scale theory result from the tremendous spatial and temporal variability in watershed characteristics and processes. A proposed step in dealing with this complexity is the development of a "globally-agreed, broad-scale catchment hydrology classification system" (McDonnell and Woods, 2004). Such a system has been widely called for to help identify underlying principles, improve model transferability, and direct experimental investigations (McDonnell and Woods, 2004; Sivapalan, 2006; Wagener et al., 2007). A number of preliminary attempts have been made to explore underlying relationships between catchments based on hydrological similarity (Hrachowitz et al., 2013; Lyon and Troch, 2010; McIntyre et al., 2005; Oudin et al., 2010, 2008; Poff et al., 2006; Post and Jones, 2001; Samaniego et al., 2010; Sawicz et al., 2011), but a unifying, process-based theory of classification remains elusive.

A classification system based on catchment function, rather than physical similarly would be intuitive and broadly beneficial (Sawicz et al., 2011). A fundamental catchment function is the collection,

storage, and discharge of precipitation (Black, 1997). The role of catchment water storage has been incorporated into runoff generation theory since at least the 1960's and development of the variable source area concept (Dunne and Black, 1970; Hewlett and Hibbert, 1967); more recently there is a large body of research describing the physical mechanisms driving non-linear runoff responses to changes in water storage at the hillslope scale (Spence, 2010, provides a recent review). There have also been several studies showing storage / discharge relationships at the catchment scale (Sayama et al., 2011; Spence et al., 2010, 2009) and a growing interest in catchment storage as an important hydrological variable (McNamara et al., 2011; Sayama et al., 2011; Spence, 2010).

One of the central challenges facing the investigation of storage / discharge relationships at the catchment scale is the difficulty, and perhaps theoretical impossibility, of measuring catchment storage. Not only is storage logistically difficult to measure, but the variable itself is sensitive to definition, and without a defined lower boundary in the soil profile is impossible to enclose. Previous studies at the catchment scale have used careful definition of estimable quantities (Spence, 2007) or monitored the change in storage (Sayama et al., 2011).

A method recently proposed in Kirchner (2009) allows derivation of watershed storage / discharge relationships without direct measurement of the storage term. In the Kirchner method, termed dynamical modeling, the relationship between storage and discharge is taken to be a function $Q = f(S)$ where Q is catchment discharge and S is catchment storage. If f is invertible and differentiable, its derivative can be written $dQ/dS = f'(f^{-1}(Q))$, which can be estimated from a time series of discharge. Kirchner (2009) found that this storage / discharge function can be used to simulate hydrographs, estimate catchment-scale evapotranspiration, precipitation, and water storage, and model recession behavior. The method gave good results for humid catchments in England (Kirchner, 2009) and Switzerland (Teuling et al., 2010) and was used to successfully measure precipitation across 24 catchments in Luxemburg (Krier et al., 2012). However, Brauer et al. (2013) found that model performance suffered in a less-humid catchments and Birkel et al. (2011) reported inconsistent estimation of dynamic storage with the method .

Dynamical modeling has the potential to address many of the research challenges outlined above. It describes a basic catchment functional attribute, explicitly incorporates non-linear storage / discharge relationships, integrates heterogeneity across the catchment scale, and provides a potentially simple mathematical form for comparison across catchment types. The goals of this study were to apply the dynamical modeling approach to a set of replicated catchment types in order to compare the modeled storage / discharge function with observed water table / discharge values and to explore similarities in model parameters as a first step towards a catchment classification system.

2.2 Materials and Methods

2.2.1 Site description

The study took place in near Juneau, Alaska. Juneau has a temperate, maritime climate, with mean annual precipitation of 1,400 mm and mean monthly temperatures ranging from -2 to 14°C. Significant rainfall occurs in all months of the year, with a pronounced increase in the fall and winter. The study sites consisted of three sub-catchment types (slope fen, forested wetland, upland) replicated across three watersheds (Fish, McGinnis, and Peterson) (Figure 2.1). The three sub-catchment types were chosen to represent a range of common hydropedologic units found in the PCTR, with the fen and forested wetland being the most commonly mapped wetland soil types and the upland representing a common, well-drained end-member. Hydropedologic units are a classification structure based around the interaction of water and soils, and provide a natural delineation in the water-dominated landscape of the PCTR (D'Amore, 2011; Lin et al., 2006). The hydropedologic units were identified using existing soil and vegetation maps and confirmed with field surveys (D'Amore, 2011).

The fen sub-catchments are located on footslope / toeslope lanforms and had deep (>1m), moderate to well decomposed peat Histosols (Typic Cryohemist). Vegetation consists of sphagnum mosses (*Sphagnum* spp.), ericaceous shrubs, and scattered sedge (*Carex* spp.) and dwarf shore pine (*Pinus contorta* var. *contorta*). All three sites have gentle (<5%) slopes towards outlet drainages.

The forested wetlands have thinner peat layers (0.5 - 1m) over glacial till, classified as Histosols (Terric Cryohemist) at the McGinnis and Fish sites and an Inceptisol (Typic Cryaquept) at the Peterson site The vegetation communities consist of sphagnum moss (*Sphagnum* spp.) and a well-developed shrub understory including both obligate wetland species such as skunk cabbage (*Lysichiton americanum*) and upland species, in particular Alaska blueberry (*Vaccenium* spp.). The overstory is mixed Sitka Spruce (*Picea sitchensis* (Bong.) Carr) and Western Hemlock (*Tsuga heterophylla* (Raf.) Sarg). Slopes are moderately higher than in the fen sites (~5% for Peterson and Fish, ~20% for McGinnis).

The upland sites are located on backslope landforms with moderately deep and moderately well-drained Spodosols (Typic or Lithic Haplocryod). These soils are thinner, with rock horizons occurring at less than 1m depth. The vegetation community is *Veccinnium* spp. dominated understory under Sitka Spruce / Western Hemlock overstory, but these forests have much higher tree basal area and volume relative to the Forested Wetlands.

2.2.2 Data collection

Discharge from each sub-catchment was monitored with a Parshall flume (Plasti-Fab, Tualatin, Oregon) instrumented with a recording stage logger (Solinst, Georgetown, Ontario) corrected for atmospheric pressure with barometric pressure transducers at each watershed. Stage was recorded at fifteen minute intervals, converted to flow using manufacturer supplied stage / discharge relationships, and aggregated to hourly values. The field sites were instrumented continuously from the summer of 2005 through the fall of 2009 with one of the watersheds (Peterson) being instrumented for the summer of 2010.

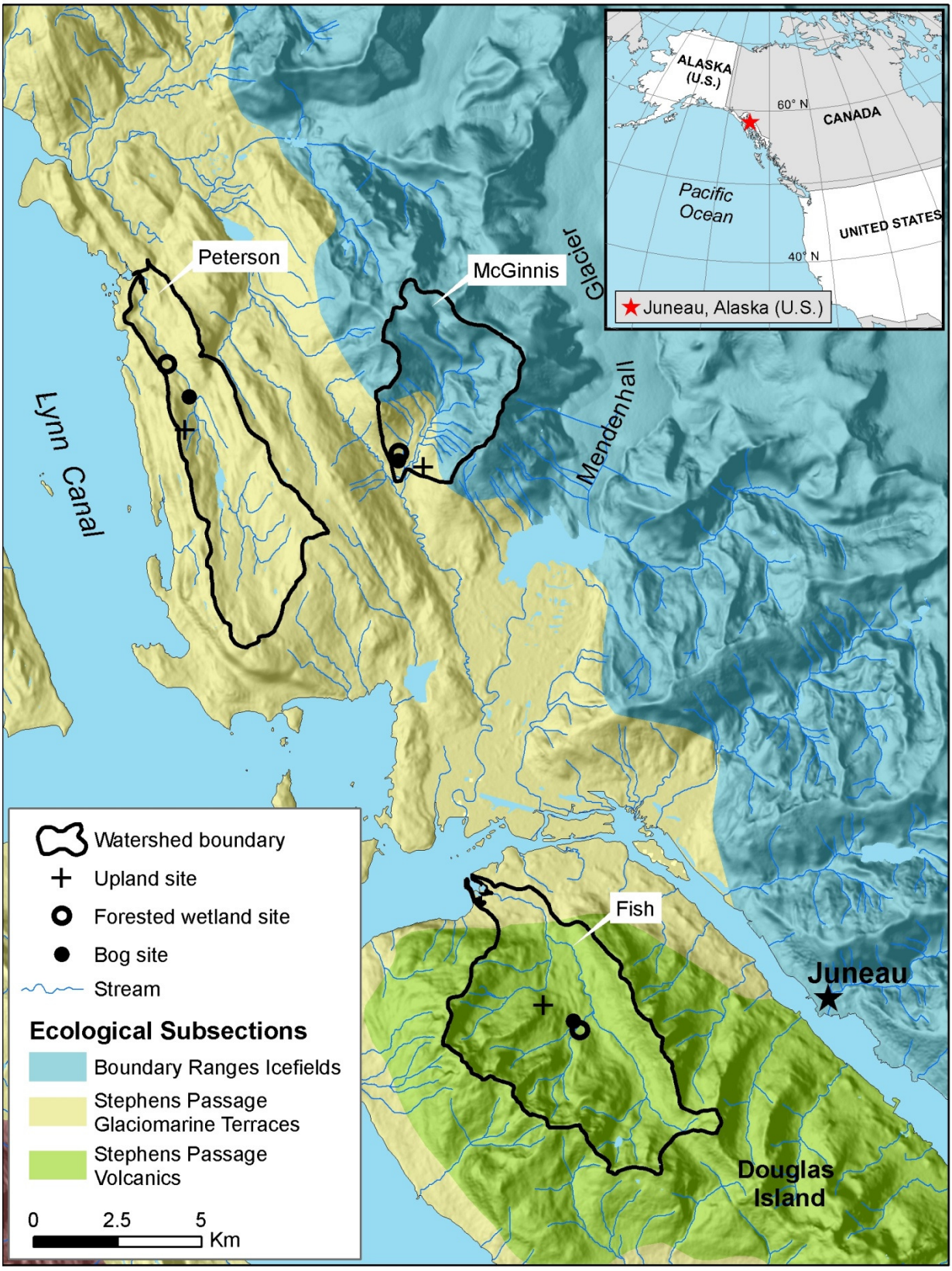

Figure 2.1. Watersheds and sub-catchments near Juneau, AK.

To avoid problems with moved flumes, frozen loggers, and inconsistent results during periods where the sites were buried under winter snowpack, the data analysis was restricted to the months of June through October for 2006 through 2010.

Hourly meteorological observations were retrieved from the National Climatic Data Center's Integrated Surface Dataset (Lott, 2004) for the Juneau Airport station (PAJK, USAF Station ID 703810). In addition, from June through October of 2013 tipping-bucket rain gauges were installed in the fen sub-catchments of the three watersheds. Hourly potential evapotranspiration (PET) was calculated using a modified Priestly-Taylor equation (Archibald and Walter, 2014) as implemented in the R package EcoHydRology (Fuka et al., 2014). This code was modified to calculate a daily atmospheric transmissivity value which was then applied to each day's hourly insolation estimation to produce hourly PET values.

2.3 Theory of dynamical modeling

The fundamental theoretical requirement of the dynamical modeling method is that discharge can be represented as a function of catchment water storage alone:

$$Q = f(S) \quad (1)$$

This definition precludes the effects of hysteresis and precipitation intensity, among others. Taking the derivative of eq. 1 with respect to time gives

$$\frac{dQ}{dt} = \frac{dQ}{dS}\frac{dS}{dt} \quad (2)$$

The change is storage dS/dt is a mass balance: the input (precipitation and / or snowmelt) minus this output (discharge and evapotranspiration)

$$\frac{dS}{dt} = P - E - Q \quad (3)$$

Substituting equation 3 into equation 2 and rearranging gives

$$\frac{dQ}{dS} = \frac{dQ/dt}{(P-E-Q)} \quad (4)$$

Where dQ/dS is the derivative of the storage discharge function $Q = f(S)$.

Selecting times when precipitation and evapotranspiration are small relative to discharge approximates dQ/*dS* as a function of Q alone

$$\frac{dQ}{dS} = g(Q) \approx \frac{-dQ/dt}{Q} \quad \Big| \quad E \ll P \ll Q \qquad (5)$$

This function *g(Q)* is termed the sensitivity function and is the solution to an ordinary, first-order non-linear differential equation. This equation can be solved to produce the storage / discharge function *f(S)* by first solving for S as a function of Q and then inverting to produce $Q = f(S)$

$$\int dS = \int \frac{dQ}{g(Q)} \qquad (6)$$

There are no restrictions of the form of *g(Q,)* and in many cases it may not be solvable analytically. The storage / discharge function can still be estimated numerically, and many of the applications of the dynamical modeling method do not require its explicit formulation.

Hydrograph simulation is achieved by combining equations 2, 3, and 4 to give

$$\frac{dQ}{dt} = g(Q)(P - E - Q) \qquad (7)$$

Equation 7 can be solved numerically to give a hydrograph given a single starting value of Q and a time series of precipitation and evapotranspiration. Additionally, the derived sensitivity function *g* can be used in the calculation of catchment-wide precipitation and evapotranspiration given a hydrograph, the estimation of catchment dynamic storage capacity, and explorations of the recession behavior of the catchment (Kirchner, 2009).

2.4 Application of dynamical modeling in the PCTR

To derive the sensitivity function, it is necessary to first identify periods when the change in storage is dominated by discharge. Two approaches proposed in Kirchner (2009) are to select periods when discharge is at least ten times larger than the sum of the magnitudes of precipitation and evapotranspiration. The second is to select nighttime periods without rainfall, assuming that in humid catchments the relative humidity at night will be high and ET fluxes will be small. Given the very short

summertime nights, persistent marine cloud layer, and cool temperatures of the PCTR the first approach was used in this study. Rainfall in the region can vary greatly over short distances and the Juneau airport record may not match precipitation at the study sites (Chapter 1), so the filter was expanded to (1) apply the precipitation and PET filter to the preceding three hours and (2) to exclude periods where discharge was rising for more than two consecutive hours. A representative hydrograph with the selected recession periods in shown in Figure 2.2.

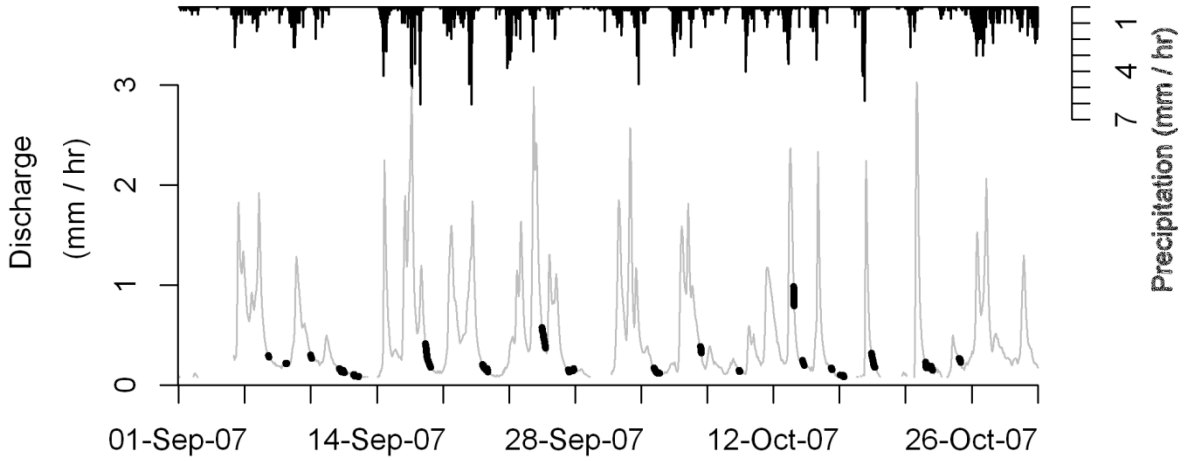

Figure 2.2. Streamflow and precipitation for the McGinnis forested wetland, 2007, with selected recession periods highlighted in black.

Once these periods of recession flow have been identified, the rate of recession if calculated as $-dQ/dt = (Q_{t-\Delta t} - Q_t) / \Delta t$ and plotted against the average discharge during that time $(Q_{t-\Delta t} + Q_t) / 2$, giving the familiar recession curve of Brutsaert and Nieber (1977) (Figure.2.3). A regression line can be fit to this plot and used to estimate the sensitivity function *g* (Equation 5). Several additional steps are introduced to improve the accuracy of estimation. First, most hydrographs span a wide range of discharge values, and the estimated sensitivity function needs to be as accurate as possible across them, so recession plots are commonly presented on log-log axes. Second, there is often considerably more scatter in $-dQ / dt$ values at low discharge values which can arise from a number of sources, including discretization of stage measurement (Rupp and Selker, 2006), missed precipitation and evapotranspiration, and greater

influence of measurement noise at low discharge. This increased variance at low discharge values could bias the regression fit. To alleviate this, I followed Kirchner (2009) by binning the individual data points and calculating a mean and standard error for $-dQ/dt$ within each bin. The bins began at the largest value of Q, covered a minimum of 1% of the logarithmic range of Q, and were allowed to expand until the standard error of $-dQ/dt$ in the bin is less than one half of its mean. Following Teuling et al. (2010) the bins were also allowed to expand if $-dQ/dt$ was negative. A regression curve was then fit to the binned averages.

There are no methodological constraints on the form of the curve fit to the binned means, other than that it be numerically integrable. Following Kirchner (2009) I used a quadratic curve fit to the log of the binned averages

$$lng(Q)) = ln(\frac{-dQ/dt}{Q}) \approx c_1 + c_2 ln(Q) + c_3 (ln(Q))^2 \quad (8)$$

Solving for $g(Q)$ gives the sensitivity function

$$g(Q) = e^{(c_1 + c_2 ln(Q) + c_3 (ln(Q))^2)} \quad (9)$$

Note that the coefficient c_2 is one less than the slope of the log-log plots, as the regression gives a function $-dQ/dt = h(Q)$ which must be divided by Q as in Equation 8..

Once the sensitivity function has been determined, it can used to simulate a hydrograph using a time series of precipitation and potential evapotranspiration. To adjust PET to approximate actual evapotranspiration, PET is multiplied by a coefficient k. This is the only tunable parameter in the hydrograph simulation; all other parameters are derived from observed data as described above. To increase numerical stability, the log transform of Equation 7 was used

$$\frac{d(ln(Q))}{dt} = \frac{1}{Q}\frac{dQ}{dt} = g(Q)(\frac{P - kE}{Q} - 1) \quad (10)$$

Numerical instability persisted in some integrations, so cf. Brauer et al. (2013) it was necessary to introduce fixed lower and upper limits of Q of 0.05 and 10 mm hr^{-1} respectively.

Available data were a discontinuous timer series covering only the summer and fall months of each year, so each year was initialized and simulated separately. The first streamflow value greater than or

equal to 0.1mm was selected as the initial value of Q, from that point on the hydrograph was simulated by the numerical solution of Equation 10. The numerical solution was calculated in R (R Core Team, 2014) using the package deSolve (Soertaert et al. 2010).

The base model for performance comparisons used a fixed one hour time step, forth order Runge-Kutta integration algorithm (method rk4). To assess the impact of *k*, the simulation was repeated with *k* values from 0 to 1 by a step size of 0.1. Simulations were performed with both a single value of *k* for all years at each site and allowing *k* to vary from year to year within a site. Model performance was assessed with the Nash-Sutcliffe efficiency (NSE) of the simulated hydrograph against observations

$$NSE = 1 - \frac{\sum_1^n (Qobs_i - Qsim_i)^2}{\sum_1^n (Qobs_i - \bar{Q})^2} \quad (11)$$

where *Qobs* and *Qsim* are observed and simulated discharge, $\bar{Q}$ is the mean of the observed *Q,* and *i* and *n* are index variables for the time period covered.

2.5 Results

Application of the filters as describe above resulted in 3-8% of the available records being useable, similar to the 8% reported in Teuling et al. (2010). The recession plots (Figure.2.3) show reasonable performance of the binning algorithm, although the McGinnis fen and upland exhibit significant scatter. The fitted regression lines are shown in Figure 2.4, coefficients for the fitted quadratic curve (Equation 8) are given in Table 2.1.

Hydrographs were simulated separately for each sub-catchment, year, and value of *k* between 0 and 1 (step 0.1). The results are shown in Table 2.2. Overall model performance was mixed, with four sites having NSE greater than zero, and a maximum of 0.45. The remaining sites have a NSE of -0.54 to -9.99. For a fixed value of *k* for all years at each site, the NSE was maximized at $k = 1$. When *k* was allowed to vary between years at each site the standard deviation for *k* between years was generally very low and again *k* was generally optimized at 1.

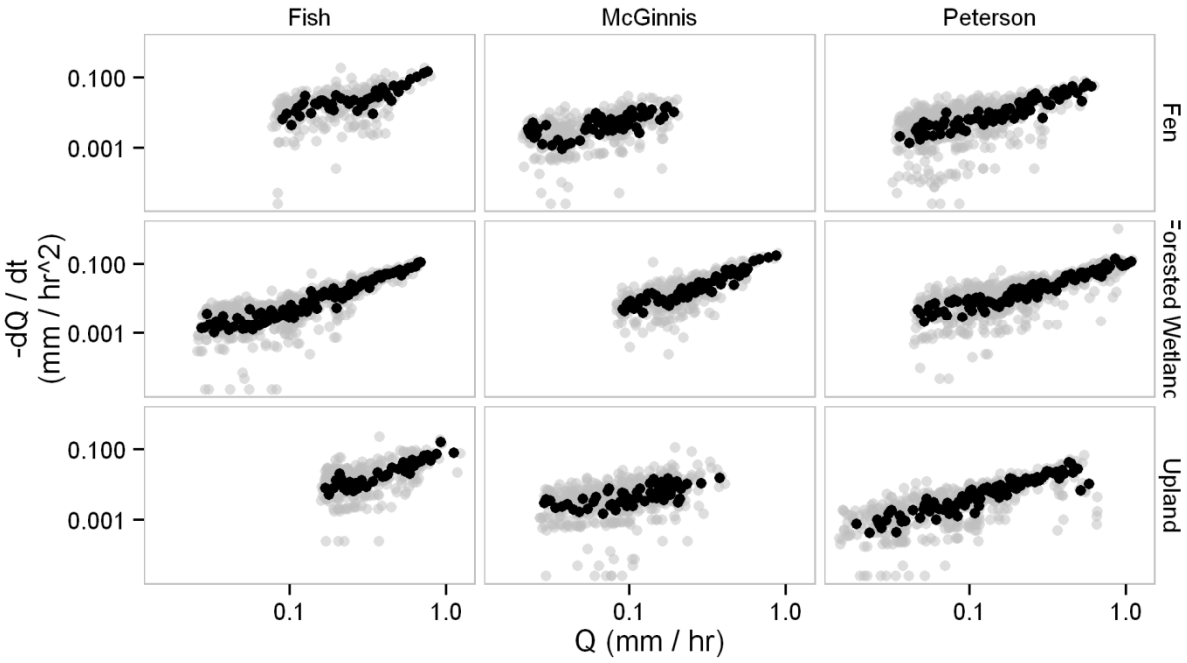

Figure.2.3. Recession plots for the nine sub-catchments. Binned averages are shown in black.

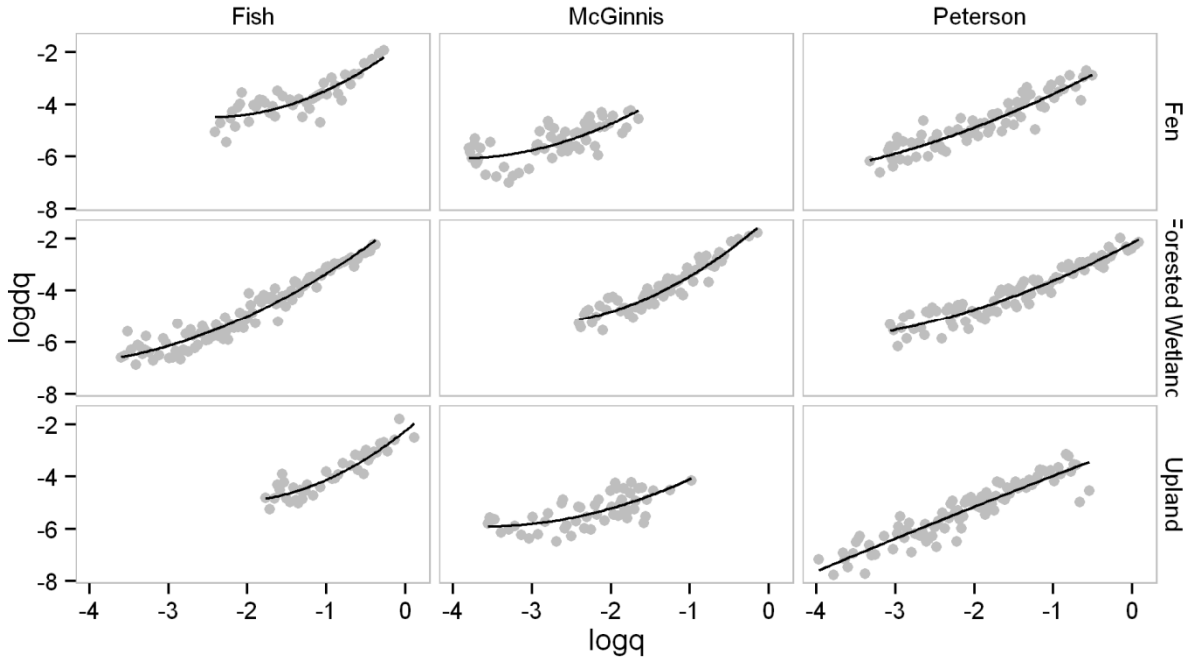

Figure 2.4. Binned averages with fitted regression lines for all sub-catchments.

Table 2.1. Coefficients for the fitted regression curves. Note that the coefficient c2 used in eq. 9 will be one less than shown here due to the Q in the denominator of Equation 8

Type	Watershed	c1	c2	c3	r2
Fen					
	Fish	-1.58	1.35	0.48	0.72
	McGinnis	-0.66	1.73	0.34	0.53
	Peterson	-2.01	0.73	0.15	0.85
Forested wetland					
	Fish	-1.18	1.41	0.25	0.94
	McGinnis	-1.21	1.68	0.44	0.90
	Peterson	-2.15	0.63	0.17	0.91
Upland					
	Fish	-2.25	1.40	0.53	0.86
	McGinnis	-2.46	0.90	0.26	0.48
	Peterson	-2.81	0.13	-0.02	0.86

Table 2.2. Summary statistics for initial model run. NSE is Nash-Sutcliffe efficiency, sd is standard deviation. RPD is the mean relative percent difference between the simulated and observed discharge values.

		fixed *k* for all years				free *k* between years		
		NSE	*k*	sd (NSE)	mean RPD	NSE	sd (*k*)	sd (NSE)
Fen								
	Fish	0.36	1	0.05	116	0.36	0.05	0.05
	McGinnis	-9.99	1	5.87	398	-9.99	0.05	5.87
	Peterson	-1.53	1	0.92	191	-1.53	0.00	0.92
Forested wetland								
	Fish	0.25	1	0.16	264	0.25	0.00	0.16
	McGinnis	0.33	1	0.11	80	0.33	0.15	0.11
	Peterson	0.45	1	0.15	141	0.45	0.42	0.15
Upland								
	Fish	-0.74	1	0.72	73	-0.74	0.30	0.61
	McGinnis	-4.72	1	4.09	255	-4.72	0.00	4.09
	Peterson	-0.54	1	0.53	316	-0.54	0.00	0.53

The relative percent difference (RPD) between the observed and simulated hydrographs was positive in all cases, showing a tendency for the model to predict higher flows than actually occurred. This can be seen in hydrographs from sites with good and poor performance (Figure 2.5).

(a)

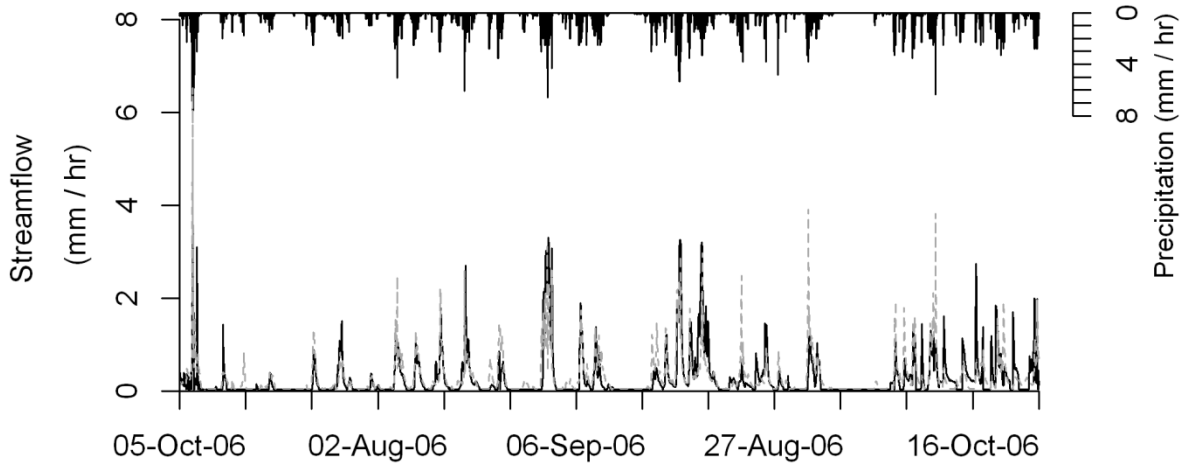

(b)

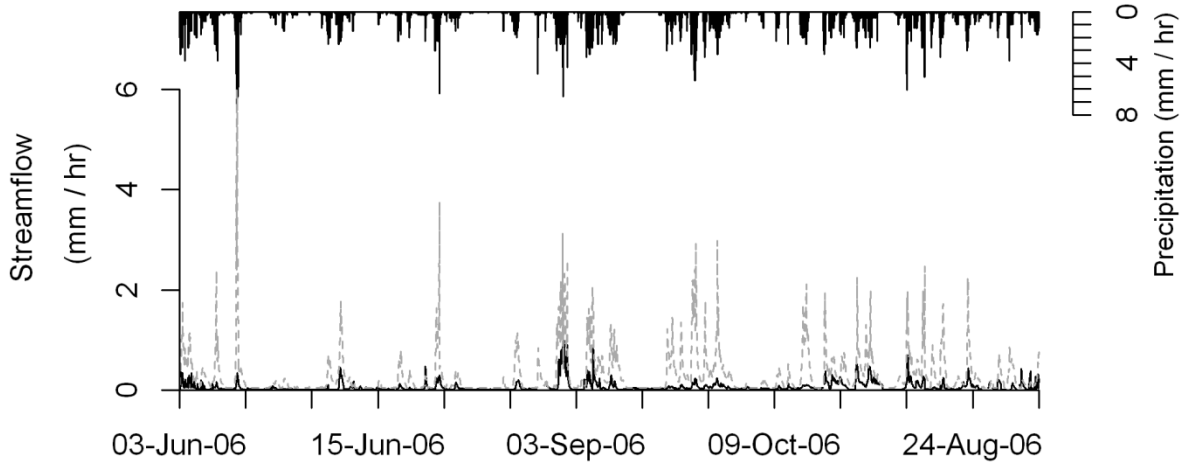

Figure 2.5 Simulated and observed hydrographs for (a) McGinnis forested wetland 2006 (NSE = 0.47), (b) McGinnis fen 2006 (NSE = -17.5). Simulated hydrograph is the dashed line.

2.6 Efforts to improve model performance

Given the poor model performance in a majority of the sub-catchments, a number of steps were taken to improve performance and identify causes of model failure. The statistic for comparison was the mean Nash-Sutcliffe efficiency (NSE) for a fixed value of *k* for all years at each sub-catchment. The results of each step are presented in Table 2.3 and Table 2.4.

2.6.1 Rupp-Selker adaptive time step in recession plotting

Rupp and Selker (2006) showed that use of a fixed time step when calculating $-dQ/dt = (Q_{t-\Delta t} - Q_t)/\Delta t$ leads to mathematical artifacts of both a high and low boundaries in recession plots. In particular, the lowest estimateable rate of decline is a function of the size of the discrete steps in stage measurement and the time step chosen. This effect can lead to large deviations from actual recession behavior at low discharge values. This can be rectified by allowing the time step to increase until a minimum ΔQ is observed

$$Q_{i-j} - Q_i \geq C[Q(H_i + \varepsilon) - Q_i] \quad (12)$$

Where $Q(H_i + \varepsilon)$ is the discharge calculated from the stage height at time i plus the minimum recordable stage increment ε, and C is an integer ≥ 1. In their analysis, Rupp and Selker (2006) showed that the value of C chosen had a strong effect on the efficacy of their method, and that the optimal value of C varied between catchments.

In this study, stage was recorded by barologgers with a step size of 0.1cm and low flows were very common, so to increase resolution at low flows the Rupp-Selker method was applied with C = 1, 5, and 10. A value of 1 for C gave the best results, and performance was improved relative to the base model. This method did not change the pattern of performance however; the same sub-catchments with positive NSE in the base model were the only sites with positive NSE, and all RPD were positive.

2.6.2 Scaled precipitation

There is considerable variation in precipitation amount over very short distances in the PCTR, with annual precipitation totals varying by as much as 50% across less than 20km in the Juneau area (NOAA 1981-2010 annual normals, cf. Arguez et al., 2012). The precipitation / PET filter was constructed to allow for differences between study sites and the Juneau airport by incorporating a three hour lag and filtering out periods of rising hydrographs. However, differences in the precipitation input for hydrograph simulation could cause serious errors.

Using a five month summertime precipitation record for the three study watersheds (Chapter 1), it was determined that precipitation totals at Fish, McGinnis, and Peterson were 106, 138, and 107% that of the Juneau Airport. As a first approximation, the hourly Juneau Airport record for the five year period of this study was multiplied by these adjustment factors and used in hydrograph simulation as in the base model. This was expected to have a particularly strong effect on the McGinnis sub-catchments, as this watershed had the highest deviation from the Juneau Airport. Performance of this model was worse across all sub-catchments, and the performance decline was particularly severe in two of the McGinnis sub-catchments with NSE changes greater than -8.

2.6.3 Optimized precipitation

There are at least two potential differences between precipitation values the sub-catchments and the Juneau airport. First, the actual precipitation received at each sub-catchment may vary substantially from the value recorded at the Juneau airport, and from the precipitation at other sub-catchments in the same watershed. Second, canopy interception and evaporation may lower the effective precipitation at sub-catchments with a forest overstory. Extending the precipitation scaling of section 2.6.2, precipitation at each sub-catchment was allowed to vary by a multiplicative coefficient p. This coefficient was varied from 0.1 to 1 by a 0.1 step, with k fixed at 0.5.

Table 2.3 Performance of modifications to the base model, part 1 of 2. Positive Nash-Sutcliffe efficiencies are shown in bold.

Type		Base model rk4	Rupp-Selker $C = 1$	Scaled precip.	Varied k		Summer only		Fall only	
	Watershed	NSE (sd)	NSE (sd)	NSE (sd)	NSE (sd)	k	NSE (sd)	k	NSE (sd)	k
Fen	Fish	**0.36** (0.05)	**0.43** (0.10)	**0.26** (0.08)	**0.36** (0.04)	1.2	-1.09 (2.35)	1	**0.46** (0.06)	1
	McGinnis	-9.99 (5.87)	-7.95 (5.11)	-19.89 (11.36)	-9.51 (5.68)	1.5	-8.87 (5.32)	0.9	-20.7 (8.64)	1
	Peterson	-1.53 (0.92)	-1.32 (0.87)	-2.49 (1.28)	-1.38 (0.86)	1.5	-5.25 (4.70)	1	-1.59 (1.00)	1
Forested wetland	Fish	**0.25** (0.16)	**0.40** (0.11)	**0.09** (0.21)	**0.27** (0.16)	1.5	-0.45 (0.53)	1	**0.35** (0.13)	1
	McGinnis	**0.33**(0.11)	**0.38** (0.11)	-0.03 (0.06)	**0.33** (0.12)	1.3	-0.06 (0.52)	1	**0.08** (0.38)	1
	Peterson	**0.45** (0.15)	**0.45** (0.15)	**0.43** (0.14)	**0.45** (0.15)	1.4	-2.76 (4.66)	1	**0.45** (0.19)	0.1
Upland	Fish	-0.74 (0.72)	-0.87(0.84)	-1.18 (0.96)	-0.71 (0.69)	1.3	-1.79 (2.20)	1	-0.62 (0.62)	1
	McGinnis	-4.72 (4.09)	-5.25 (4.23)	-13.03 (9.79)	-4.43 (3.94)	1.5	-11.77 (10.06)	1	-7.52 (4.31)	1
	Peterson	-0.54 (0.53)	-0.52 (0.50)	-0.99 (0.68)	-0.45 (0.52)	1.5	-2.84 (3.88)	1	-1.61 (2.50)	1
Mean		-1.79	-1.58	-4.09	-1.67		-3.88		-3.41	

Table 2.4 Performance of modifications to the base model, part 2 of 2. Positive Nash-Sutcliffe efficiencies are shown in bold.

Type		Base model rk4	Bypassing flow			Optimized precip.	
	Watershed	NSE (sd)	NSE (sd)	*k*	*kp*	NSE (sd)	*p*
Fen	Fish	**0.36** (0.05)	**0.36** (0.05)	1	0	**0.37** (0.08)	0.8
	McGinnis	-9.99 (5.87)	-10.01 (5.61)	1	0	**0.22** (0.17)	0.2
	Peterson	-1.53 (0.92)	-1.69 (0.99)	1	0	**0.55** (0.12)	0.5
Forested wetland	Fish	**0.25** (0.16)	**0.24** (0.15)	1	0	**0.40** (0.06)	0.7
	McGinnis	**0.33**(0.11)	**0.32** (0.10)	1	0.01	**0.22** (0.19)	0.8
	Peterson	**0.45** (0.15)	**0.44** (0.14)	1	0	**0.43** (0.15)	1.0
Upland	Fish	-0.74 (0.72)	-0.79 (0.81)	1	0	-0.12 (0.36)	0.7
	McGinnis	-4.72 (4.09)	-5.04 (4.01)	1	0	**0.41** (0.20)	0.5
	Peterson	-0.54 (0.53)	-0.64 (0.54)	1	0	**0.27** (0.16)	0.4
		-1.79	-1.86			**0.32**	

Model performance was substantially improved, with NSE values as high as 0.55 and positive values at all but one sub-catchment. However, several features prevent clear extrapolation to the physical system. First, the sub-catchments that performed the worst with the base model had the largest changes to precipitation input and very low values of p (0.2 to 0.4). While some variation in rainfall is known to occur, it is extremely unlikely that precipitation values vary by a factor of 4 between study watersheds. Because the model consistently over-estimates discharge, any adjustment that lowers simulated streamflow will improve performance, but it may be masking errors in other parts of the model. Second, there is implausible variation between sub-catchments within the same watershed. For example, the McGinnis fen and forested wetland are within 200m of one another and gave optimal values of $p = 0.2$ and 0.8, respectively. Third, the pattern in optimal p values does not match what would be expected from canopy interception; values in the fens are quite low relative to the forested wetlands and uplands, as in the McGinnis example above. Finally, the scaled precipitation values for the fens do not follow the pattern observed from direct measurement (see section 2.6.2). The watershed with the highest observed precipitation relative to the airport (McGinnis, 137%) had the lowest optimal value of p (0.2). Allowing precipitation to vary does help to correct problems of over-estimation of flow, but it does not appear that differential precipitation values are responsible for poor model performance.

2.6.4 Expanded PET values

All models have consistently selected $k = 1$ as the optimal value and have consistently overestimated flows. PET was estimated via a modification of the Priestly-Taylor equation, and as errors in estimation are not necessarily one sided it is possible that estimated PET is lower than actual ET. The hydrograph simulation was run allowing k to vary from 0 to 1.5 by 0.1. While performance was improved relative to the base model, gains were modest ($\Delta NSE < 0.1$). Optimal values of k were all greater than 1 and all RPD were positive, again showing persistent over-estimation of discharge. As was the case with precipitation, reduction of discharge via increased ET may be masking errors elsewhere in the model

2.6.5 Separation into seasons.

For the dynamical modeling approach to succeed, it is necessary that the catchments are hydrologically closed (Equation 3). Soils in the PCTR are generally very wet, with water tables in the fens and forested wetlands never dropping below 50cm from the surface and frequently saturating almost completely (Chapter 1). Combined with the steep topography in the region, there is potential for water movement across sub-catchment boundaries via subsurface flow. Water tables show a distinct seasonality and are significantly higher in the fall months (Sep-Oct) compared to the summer (June-July-August) (Chapter 1). Increased saturation could potentially activate sub-surface flow pathways, degrading model performance. To test for this effect, the available data were split into summer and fall datasets. Each dataset was used to derive a sensitivity function and simulate the hydrographs for the season it was derived from. If seasonal increases in soil moisture were reducing hydrological closure, performance in the dry summer months would be expected to be better than in the wet fall.

Relative to the base model, performance in summer was worse across all sub-catchments, with the exception of a modest improvement in the highly negative NSE at one site. Performance in the fall was mixed. Sub-catchments that performed well in the base model generally saw modest performance increases; models that performed poorly in the base model were generally degraded. A clear pattern is not apparent, and the effects seen do not support the theory of increasingly porous sub-catchment boundaries in the fall.

2.6.6 Bypassing flow

A central assumption of the dynamical modeling approach is that discharge depends solely on catchment storage. However, in some cases precipitation may be routed directly to the output and bypass catchment storage, for example overland flow, macropore flow, or precipitation directly into the stream channel. This bypassing flow can be accommodated into the dynamical model by the inclusion of a bypass coefficient so that the storage / discharge function becomes

$$Q = f(S) + k_p P \quad (13)$$

Leading to

$$\frac{dQ}{dt} = \frac{dQ}{dS}\frac{dS}{dt} + k_p\frac{dP}{dt} = g\left(Q - k_p\right)(P - E - Q) + k_p\frac{dP}{dt} \quad (14)$$

Much like k, value of k_p can be optimized to maximize NSE. Hydrographs were simulated for all sub-catchments as in the base model, with the addition of the k_p term in eq. 12. Values of k and k_p were varied independently, k from 0 to 1 by 0.1 and k_p from 0 to 0.1 by 0.01, and then from 0.1 to 1 by 0.1.

Performance was very similar to the base model. Values of k were always optimized at 1, and k_p at or near 0, making the model mathematically approximate the base model (slight deviations in NSE from the base model result from the need to constrain ($Q - k_p$) to positive values for calculation). As in the base model all RPD were positive.

2.7 Model assessment

Attempts to improve model performance did not lead to satisfactory outcomes; the maximum NSE for any site was 0.55, and only the scaled precipitation (section 2.6.3) gave positive NSE for more than four of the nine sub-catchments. The same sub-catchments consistently gave the best performance (the forested wetlands and Fish fen). Discharge was over-estimated in almost every simulation, and when parameters with the potential to reduce discharge were included (k, p) their values were optimized in the direction of discharge reduction. As such, there appear to be systematic problems with the dynamical modeling approach at five of the nine sub-catchments, and persistent over-estimation of discharge flow in all catchments, especially those with poor model performance.

2.7.1 Catchment size constraints

To help identify the simulation error and examine the plausibility of observed and simulated catchment behavior, we estimated constraints on catchment size assuming (1) all precipitation was routed to discharge, giving the smallest possible catchment or (2) measured discharge was equal to precipitation

minus PET, giving the largest catchment estimate.

$$Area_{max} = \frac{Q}{p} \quad (15)$$

$$Area_{min} = \frac{Q}{p-PET} \quad (16)$$

Where Q is volumetric discharge (m^3) and p and PET are precipitation and potential evapotranspiration as depth (m).Discharge and precipitation data were taken from the 2013 dataset (Chapter 1) because of the availability of precipitation measurements in each watershed. The sensitivity function derived from the 2005-2010 dataset was used to simulate 2013 discharge as in section 2.4. Because of the observed discharge term, estimates of catchment size are sensitive to the discharge value assigned to low-censored observations, so an error range is given to encompass estimates assigning values of 0 and the censoring limit to these observations.

Of the nine sub-catchments, two had measured sizes that fell in the range of calculated sizes, two had measured areas within 5% of their calculated maximum, and the remaining four had measured sizes 25 to 140% larger than their calculated maximum (Table 2.5). The four sub-catchments with consistently reasonable model performance had measured sizes either within their calculated range or within 5% of their maximum. The five sub-catchments with consistently poor model performance had measured areas 41% to 74% larger than their calculated maximum.

Modeled discharge was greater than observed discharge in all sub-catchments. In the four reasonably modeled sub-catchments simulated discharge was 12% to 69% higher than observed. In the five poorly-modeled sub-catchments simulated discharge was173% to 229% higher than observed. Observed runoff ratios were 59-88% for the reasonably-modeled sites and 17-41% for the poorly-modeled sites. Taken together, these results suggest that there are alternative routes of water loss from sub-catchments with poor model performance.

2.7.2 Potential subsurface flow

The magnitude of the loss via the alternative flow routes can be estimated by closing the mass balance with an additional loss term and rearranging to give

$$l = p - PET - q \quad (16)$$

Where l is the loss term (m) and p, PET, and q are precipitation, PET, and discharge, all as depth (m) over the measured catchment size. This loss term can then be adjusted by the time period to produce an average rate. The average loss rates for the five sub-catchments with substantially over-estimated maximum catchment sizes and poor model performance varied from 1.4 to 3.6 mm day^{-1} (Table 2.5).

For the two fen sub-catchments, slow lateral flow could be occurring through the deep peat layers. Although conductivity in decomposed peat is generally low, the substantial depth of these profiles could still lead to considerable water loss. As an approximation, we can consider the peat to be 3.5m deep (D'Amore, personal communication), flow to be occurring across a width equal to the diameter of the catchment area expressed as a circle, and a slope of 5%.We can then estimate the flow rate using a simplified form of Darcy's law

$$k = \frac{L}{A\frac{dh}{dl}} \quad (17)$$

where k is the flow rate (m s^{-1}), L is the volumetric water loss (m^3 s^{-1}), A is the cross-sectional area of flow (m^2), and dh/dl is the slope (%). In the upland catchments, water may be lost to fractured bedrock at the base of the soil profile. All upland sub-catchments soil profiles terminate in rock at less than 1m depth. As an approximation, we can consider the loss term to consist solely of flow into this rock layer. Ignoring the effects of hydrostatic pressure and matrix potential, we can divide the loss term by the catchment area to estimate the rate of flow into the bedrock, providing a minimum necessary saturated hydraulic conductivity. Doing so gives estimates of flow rate of 1.5 x 10^{-8} to 3.6 x 10^{-8} m s^{-1}, again well within the plausible rates of flow for these systems.

Table 2.5 Catchment size calculations, moisture balance, and loss rate estimation. Errors in catchment size are associated with values assigned to low-censored observations. q_{sim} is simulated discharge, q_{obs} is observed discharge, and precip is precipitation. RPD is the relative percent difference between the measured and calculated maximum catchment areas. Positive NSE shown in bold. Loss calculations not performed for catchments with measured sizes within their calculated ranges.

		Catchment size				Base model					
	site	small	measured	large	RPD	NSE	q_{sim}/ precip	q_{sim}/ q_{obs}	q_{obs} / precip	loss rate (mm day^{-1})	loss flow rate m s^{-1}
Fen	Fish	1.02 ± 0.09	1.52	1.77 ± 0.16	na	**0.42**	1.06	1.57	67	na	
	McGinnis	0.36 ± 0.03	2.07	0.56 ± 0.05	73	-8.21	0.57	3.29	17	3.6	6.11E-05
	Peterson	0.4 ± 0.03	1.28	0.69 ± 0.05	46	-1.37	0.96	3.06	31	1.6	2.07E-05
Forested wetland	Fish	7.66 ± 0.25	13.08	12.85 ± 0.42	2	**0.4**	0.99	1.69	59	< 0.1	2.66E-06
	McGinnis	2.79 ± 0.26	4.27	4.15 ± 0.39	3	**0.36**	1.01	1.54	65	0.1	3.53E-06
	Peterson	2.33 ± 0.09	2.64	3.99 ± 0.16	na	**0.45**	0.99	1.12	88	na	
Upland	Fish	2.26 ± 1.52	5.56	3.14 ± 2.11	44	-1.24	1.24	3.06	41	1.9	2.22E-08
	McGinnis	0.52 ± 0.02	1.64	0.74 ± 0.02	55	-5.43	0.97	3.03	32	3.0	3.48E-08
	Peterson	8.03 ± 0.29	23.69	14.02 ± 0.5	41	-0.52	0.93	2.73	34	1.4	1.59E-08

2.7.3 Comparison with observed water table / discharge data

Chapter 1 demonstrated a strong, non-linear water table / discharge relationship in the fen and forested wetland sites and in one of the upland sub-catchments (Figure 1.9). Correlation of modeled storage / discharge relationships with the observed water table record requires (1) an appropriate integration constant to locate the storage / discharge curve and (2) a translation between storage depth and water table position. As a first approximation, an integration constant was chosen for each sub-catchment so that the simulated discharge equal to the maximum observed discharge occurred at the maximum observed water table. To translate modeled storage to observed water table a porosity of 90% for the organic soils and 75% for the mineral soils was used. Measured bulk densities in the upper mineral horizons are relatively low (0.3 – 0.5 gm cm^{-3}), making this high porosity reasonable. The results are shown in Figure 2.6. Agreement between observations and the model is fair in the fens are forested wetlands, showing a strong, non-linear response to increasing storage. Notably, the fit is poor in the Peterson forested wetland, which consistently gave the highest NSE values. Agreement is also poor in the uplands, where the model predicts higher rates of discharge than observed and fails to capture the threshold dynamics in the Peterson site. Caution should be exercised in interpreting these results, as model performance in hydrograph simulation indicates that the models were not fully capturing the catchment behavior.

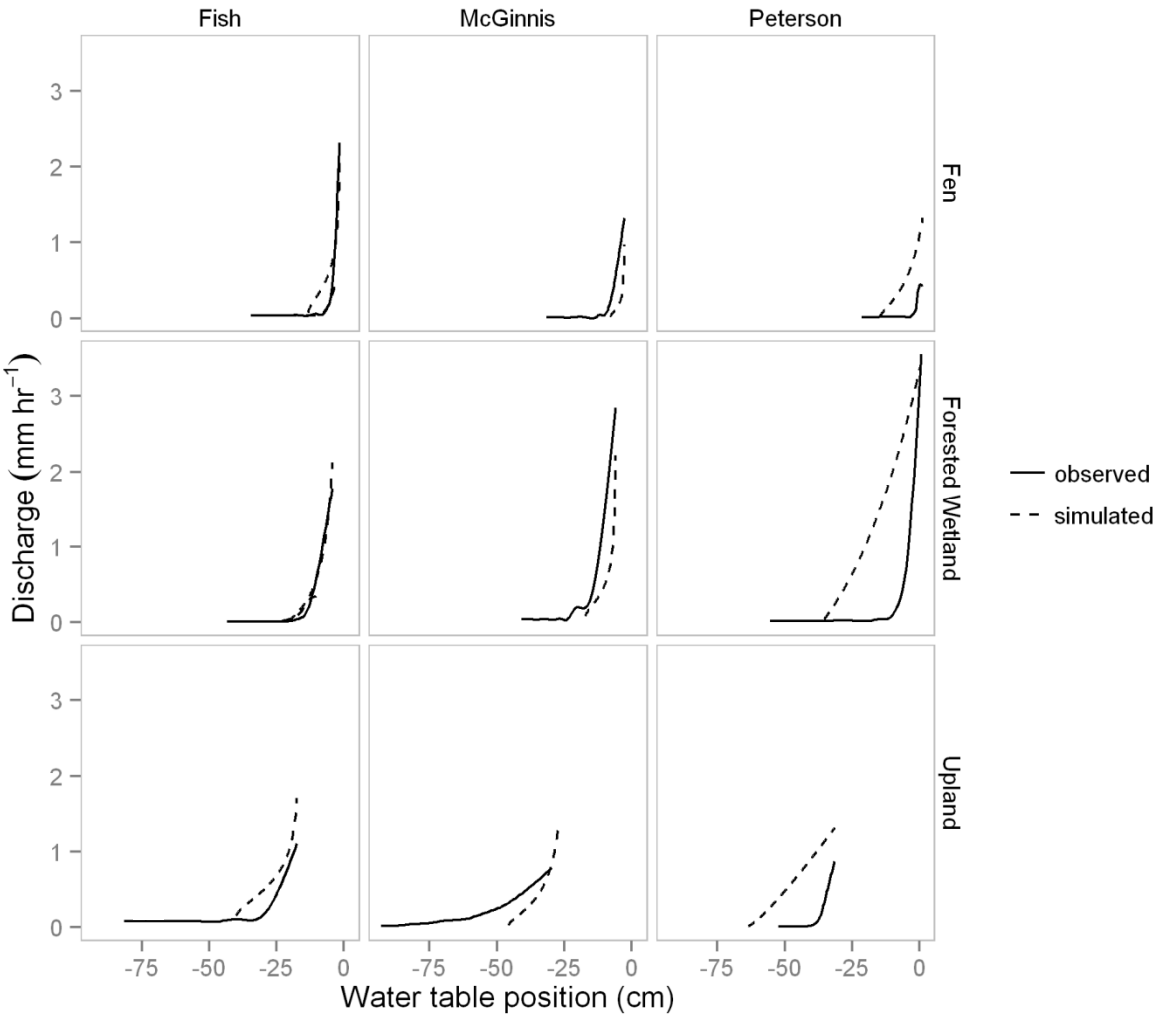

Figure 2.6. Observed and modeled water table / discharge relationships. The solid line is a loess smooth fitted to the water table / discharge data from 2013 (Chapter 1, Figure 1.9). The dashed line is the simulated relationship based on storage / discharge functions derived from the dataset presented in chapter 2.

2.8 Discussion

Model performance was generally very poor for five of the nine sub-catchments, and consistently better for the remaining four. The best, physically plausible performance was obtained using a fixed time step fourth order Runge-Kutta integration and a Rupp-Selker variable time step recession plot with an error coefficient *C* of one. Persistent overestimation of discharge and catchment water balances suggested that sub-catchments with poor performance were discharging water through un-accounted for flow

pathways, most likely in the subsurface. The average rate of loss in these systems was shown to be broadly consistent with lateral subsurface flow through the deep peat in the fens and into fractured bedrock in the uplands.

Although hydrograph simulation using the dynamical model did not adequately capture catchment behavior across all sites, it did show broadly consistent agreement with measured water table / discharge relationships, particularly the fens and forested wetlands. Improved procedures to align the numerically integrated storage / discharge functions with physical properties, particularly in catchments without available soil water data, is an important direction of future research.

In this study, poor model performance precluded the planned additional step of examining model structure for similarities between sub-catchment types. Nevertheless, the technique remains promising if it can be shown to capture a broad range of watershed storage / discharge functions. Most studies to date using this method have followed (Kirchner, 2009) and used a quadratic function fit to logarithms to estimate the derivative of the function *f,* other model formulations to allow more informative catchment comparison remain unexplored.

3 Conclusion

Runoff generation in wet soils of the northern Pacific perhumid coastal temperate rainforest occurs as a strong, non-linear response to soil water table position. Precipitation inputs that fail to raise the water table to this critical level produce very little runoff. Once the threshold is passed, runoff increases rapidly and further water table rise is limited as additional water inputs are routed to discharge. In the wet soils this discharge threshold occurs in the upper soil profile; within the top 10cm in the fens and from a depth of 20cm to 10cm in the forested wetlands. There is some evidence that this hydrologically active zone corresponds to increased fiber content and decreased peat development. Discharge in the well-drained upland catchments shows more variation, with a threshold response occurring in some study sites and a more linear response in others. The water table and runoff dynamics of these upland sites appears to be controlled by the underlying rock horizons. In all sites, both total precipitation and antecedent water table position are strong predictors of runoff generation.

Despite abundant summer rainfall and cool temperatures, there is a pronounced seasonal decline in catchment moisture balances in the PCTR, with potential evapotranspiration exceeding precipitation for several months during the summer. During this time, water tables in all sub-catchment types declined, as did catchment runoff ratios. Catchment moisture balances are determined by the interaction of PET and precipitation, with the precipitation term dominating in the PCTR. The regional climate is projected to become warmer and seasonally wetter, and as these changes affect moisture balance they have the potential to cause non-linear responses in runoff generation and biogeochemical processing.

An attempt was made to capture this threshold response by modeling catchment discharge as a function of storage using a first-order, ordinary differential equation. Model performance was reasonable for four of the sub-catchments and very poor for the remaining five. Adjustments to the model that reduced simulated discharge improved performance, but the effective adjustments were physically implausible and were most likely compensating for problems elsewhere in the model. The patterns of

model performance were persistent, with the same four sub-catchments generally doing well and the rest poorly, Modeled discharge was consistently higher than observations.

Estimating maximum catchment size on the basis of a mass balance showed that the five poorly performing models were considerably larger than their maximum estimated size, suggesting the presence of an additional discharge pathway. The magnitude of this pathway was estimated using a water mass balance, and two potential physical mechanisms were proposed: lateral flow through the peat profile in the fens, and vertical flow into bedrock in the uplands. In both cases, a simple approximation of flow rates was shown to be within known ranges of hydraulic properties in similar systems.

Although the modeled storage / discharge functions did not fully capture hydrological performance in all sub-catchments, an initial effort to correlate the functions with the water table / discharge relationships from chapter 1 showed promise. Agreement was good in the fens and forested wetlands, with one exception, and poorer in the uplands. Poor overall model performance prevents a definitive assessment of the correlation methods, but the results shown should encourage further work.

4 References

Alaback, P.B., 1991. Comparative ecology of temperate rainforests of the Americas along analogous climatic gradients. Rev. Chil. Hist. Nat. 64, 399–412.

Alaback, P.B., 1996. Biodiversity Patterns in Relation to Climate: The Coastal Temperate Rainforests of North America, in: Lawford, R.G., Fuentes, E., Alaback, P.B. (Eds.), High-Latitude Rainforests and Associated Ecosystems of the West Coast of the Americas, Ecological Studies. Springer New York, pp. 105–133.

Alvarez-Cobelas, M., Angeler, D.G., Sánchez-Carrillo, S., Almendros, G., 2010. A worldwide view of organic carbon export from catchments. Biogeochemistry 107, 275–293. doi:10.1007/s10533-010-9553-z

Archibald, J.A., Walter, M.T., 2014. Do Energy-Based PET Models Require More Input Data than Temperature-Based Models? — An Evaluation at Four Humid FluxNet Sites. JAWRA J. Am. Water Resour. Assoc. 50, 497–508. doi:10.1111/jawr.12137

Arguez, A., Durre, I., Applequist, S., Vose, R.S., Squires, M.F., Yin, X., Heim, R.R., Owen, T.W., 2012. NOAA's 1981–2010 U.S. Climate Normals: An Overview. Bull. Am. Meteorol. Soc. 93, 1687–1697. doi:10.1175/BAMS-D-11-00197.1

Bay, R.R., 1969. Runoff from small peatland watersheds. J. Hydrol. 9, 90–102.

Beven, K., 2006. A manifesto for the equifinality thesis. J. Hydrol., The model parameter estimation experiment MOPEX MOPEX workshop 320, 18–36. doi:10.1016/j.jhydrol.2005.07.007

Beven, K.J., 2001. Dalton Medal Lecture: How far can we go in distributed hydrological modelling? Hydrol. Earth Syst. Sci. 5, 1–12.

Birkel, C., Soulsby, C., Tetzlaff, D., 2011. Modelling catchment-scale water storage dynamics: reconciling dynamic storage with tracer-inferred passive storage. Hydrol. Process. 25, 3924–3936. doi:10.1002/hyp.8201

Black, P.E., 1997. Watershed Functions. JAWRA J. Am. Water Resour. Assoc. 33, 1–11. doi:10.1111/j.1752-1688.1997.tb04077.x

Brauer, C.C., Teuling, A.J., Torfs, P.J.J.F., Uijlenhoet, R., 2013. Investigating storage-discharge relations in a lowland catchment using hydrograph fitting, recession analysis, and soil moisture data: Storage-Discharge Relations in a Lowland Catchment. Water Resour. Res. 49, 4257–4264. doi:10.1002/wrcr.20320

Brutsaert, W., Nieber, J.L., 1977. Regionalized drought flow hydrographs from a mature glaciated plateau. Water Resour. Res. 13, 637–643. doi:10.1029/WR013i003p00637

Bryant, M.D., 2009. Global climate change and potential effects on Pacific salmonids in freshwater ecosystems of southeast Alaska. Clim. Change 95, 169–193. doi:10.1007/s10584-008-9530-x

Clymo, R.S., 1984. The Limits to Peat Bog Growth. Philos. Trans. R. Soc. B Biol. Sci. 303, 605–654. doi:10.1098/rstb.1984.0002

Cowardin, L.M., Carter, V., Golet, F.C., LaRoe, E.T., 1979. Classification of wetlands and deepwater habitats of the United States. Fish and Wildlife Service, US Department of the Interior Washington, DC.

D'Amore, D., 2011. Hydrologic Controls on Carbon Cycling in Alaskan Coastal Temperate Rainforest Soils (Dissertation). University of Alaska, Fairbanks, AK.

Dahlke, H.E., Easton, Z.M., Walter, M.T., Steenhuis, T.S., 2012. Field test of the variable source area interpretation of the curve number rainfall-runoff equation. J. Irrig. Drain. Eng. 138, 235–244.

Daniels, S.M., Agnew, C.T., Allott, T.E.H., Evans, M.G., 2008. Water table variability and runoff generation in an eroded peatland, South Pennines, UK. J. Hydrol. 361, 214–226. doi:10.1016/j.jhydrol.2008.07.042

Davidson, E.A., Janssens, I.A., 2006. Temperature sensitivity of soil carbon decomposition and feedbacks to climate change. Nature 440, 165–173. doi:10.1038/nature04514

DellaSala, D.A., Alaback, P., Spribille, T., Wehrden, H. von, Nauman, R.S., 2011. Just What Are Temperate and Boreal Rainforests?, in: Temperate and Boreal Rainforests of the World: Ecology and Conservation. Island Press/Center for Resource Economics, pp. 1–41.
Devito, K.J., Hill, A.R., Roulet, N., 1996. Groundwater-surface water interactions in headwater forested wetlands of the Canadian Shield. J. Hydrol. 181, 127–147. doi:10.1016/0022-1694(95)02912-5
Dooge, J.C.I., 1986. Looking for hydrologic laws. Water Resour. Res. 22, 46S–58S. doi:10.1029/WR022i09Sp0046S
Dunne, T., Black, R.D., 1970. An experimental investigation of runoff production in permeable soils. Water Resour. Res. 6, 478–490.
Edwards, R.T., D'Amore, D.V., Hood, E., 2007. Regional DOC Fluxes for the Tongass National Forest in Southeast Alaska. AGU Fall Meet. Abstr. -1, 0754.
Emili, L.A., Price, J.S., 2006. Hydrological processes controlling ground and surface water flow from a hypermaritime forest–peatland complex, Diana Lake Provincial Park, British Columbia, Canada. Hydrol. Process. 20, 2819–2837. doi:10.1002/hyp.6077
Emili, L.A., Price, J.S., Fitzgerald, D.F., 2006. Hydrogeological influences on forest community type along forest–peatland complexes in coastal British Columbia. Can. J. For. Res. 36, 2024–2037. doi:10.1139/x06-104
Evans, M.G., Burt, T.P., Holden, J., Adamson, J.K., 1999. Runoff generation and water table fluctuations in blanket peat: evidence from UK data spanning the dry summer of 1995. J. Hydrol. 221, 141–160.
Fellman, J.B., Hood, E., Edwards, R.T., D'Amore, D.V., 2009. Changes in the concentration, biodegradability, and fluorescent properties of dissolved organic matter during stormflows in coastal temperate watersheds. J. Geophys. Res. 114. doi:10.1029/2008JG000790
Fitzgerald, D.F., Price, J.S., Gibson, J.J., 2003. Hillslope-swamp interactions and flow pathways in a hypermaritime rainforest, British Columbia. Hydrol. Process. 17, 3005–3022. doi:10.1002/hyp.1279
Ford, J., Bedford, B.L., 1987. The Hydrology of Alaskan Wetlands, U.S.A.: A Review. Arct. Alp. Res. 19, 209. doi:10.2307/1551357
Fuka, D.R., Walter, M.T., Archibald, J.A., Steenhuis, T.S., Easton, Z.M. (2014). EcoHydRology: A community modeling foundation for Eco-Hydrology. Rpackage version 0.4.12. http://CRAN.R-project.org/package=EcoHydRology
Graham, C.B., McDonnell, J.J., 2010. Hillslope threshold response to rainfall: (2) Development and use of a macroscale model. J. Hydrol. 393, 77–93. doi:10.1016/j.jhydrol.2010.03.008
Heath, L.S., Smith, J.E., Woodall, C.W., Azuma, D.L., Waddell, K.L., 2011. Carbon stocks on forestland of the United States, with emphasis on USDA Forest Service ownership. Ecosphere 2, art6. doi:10.1890/ES10-00126.1
Hewlett, J.D., Hibbert, A.R., 1967. Factors affecting the response of small watersheds to precipitation in humid areas. For. Hydrol. 275–290.
Hinton, M.J., Schiff, S.L., English, M.C., 1998. Sources and flowpaths of dissolved organic carbon during storms in two forested watersheds of the Precambrian Shield. Biogeochemistry 41, 175–197.
Holden, J., 2005. Peatland hydrology and carbon release: why small-scale process matters. Philos. Trans. R. Soc. Math. Phys. Eng. Sci. 363, 2891–2913. doi:10.1098/rsta.2005.1671
Holden, J., Burt, T.P., 2003. Runoff production in blanket peat covered catchments. Water Resour. Res. 39, n/a–n/a. doi:10.1029/2002WR001956
Holden, J., Burt, T.P., 2003. Hydrological studies on blanket peat: the significance of the acrotelm-catotelm model. J. Ecol. 91, 86–102.
Hood, E., Gooseff, M.N., Johnson, S.L., 2006. Changes in the character of stream water dissolved organic carbon during flushing in three small watersheds, Oregon. J. Geophys. Res. Biogeosciences 111, G01007. doi:10.1029/2005JG000082

Hornberger, G.M., Bencala, K.E., McKnight, D.M., 1994. Hydrological controls on dissolved organic carbon during snowmelt in the Snake River near Montezuma, Colorado. Biogeochemistry 25, 147–165. doi:10.1007/BF00024390

Hrachowitz, M., Savenije, H.H.G., Blöschl, G., McDonnell, J.J., Sivapalan, M., Pomeroy, J.W., Arheimer, B., Blume, T., Clark, M.P., Ehret, U., Fenicia, F., Freer, J.E., Gelfan, A., Gupta, H.V., Hughes, D.A., Hut, R.W., Montanari, A., Pande, S., Tetzlaff, D., Troch, P.A., Uhlenbrook, S., Wagener, T., Winsemius, H.C., Woods, R.A., Zehe, E., Cudennec, C., 2013. A decade of Predictions in Ungauged Basins (PUB)—a review. Hydrol. Sci. J. 58, 1198–1255. doi:10.1080/02626667.2013.803183

Ingram, H. a. P., 1978. Soil Layers in Mires: Function and Terminology. J. Soil Sci. 29, 224–227. doi:10.1111/j.1365-2389.1978.tb02053.x

Kirchner, J.W., 2009. Catchments as simple dynamical systems: Catchment characterization, rainfall-runoff modeling, and doing hydrology backward. Water Resour. Res. 45, n/a–n/a. doi:10.1029/2008WR006912

Krier, R., Matgen, P., Goergen, K., Pfister, L., Hoffmann, L., Kirchner, J.W., Uhlenbrook, S., Savenije, H.H.G., 2012. Inferring catchment precipitation by doing hydrology backward: A test in 24 small and mesoscale catchments in Luxembourg: UNDERSTANDING HYDROLOGY BACKWARD. Water Resour. Res. 48, n/a–n/a. doi:10.1029/2011WR010657

Lai, D.Y.F., 2009. Methane dynamics in northern peatlands: a review. Pedosphere 19, 409–421.

Leighty, W.W., Hamburg, S.P., Caouette, J., 2006. Effects of Management on Carbon Sequestration in Forest Biomass in Southeast Alaska. Ecosystems 9, 1051–1065. doi:10.1007/s10021-005-0028-3

Letts, M.G., Roulet, N.T., Comer, N.T., Skarupa, M.R., Verseghy, D.L., 2000. Parametrization of peatland hydraulic properties for the Canadian land surface scheme. Atmosphere-Ocean 38, 141–160. doi:10.1080/07055900.2000.9649643

Lin, H., Bouma, J., Pachepsky, Y., Western, A., Thompson, J., van Genuchten, R., Vogel, H.-J., Lilly, A., 2006. Hydropedology: Synergistic integration of pedology and hydrology: OPINION. Water Resour. Res. 42, n/a–n/a. doi:10.1029/2005WR004085

Lott, J.N., 2004. 7.8 THE QUALITY CONTROL OF THE INTEGRATED SURFACE HOURLY DATABASE.

Lyon, S.W., Seibert, J., Lembo, A.J., Walter, M.T., Steenhuis, T.S., 2006. Geostatistical investigation into the temporal evolution of spatial structure in a shallow water table. Hydrol. Earth Syst. Sci. Discuss. 10, 113–125.

Lyon, S.W., Troch, P.A., 2010. Development and application of a catchment similarity index for subsurface flow. Water Resour. Res. 46, W03511. doi:10.1029/2009WR008500

Mantua, N., Tohver, I., Hamlet, A., 2010. Climate change impacts on streamflow extremes and summertime stream temperature and their possible consequences for freshwater salmon habitat in Washington State. Clim. Change 102, 187–223. doi:10.1007/s10584-010-9845-2

McDonnell, J.J., Sivapalan, M., Vaché, K., Dunn, S., Grant, G., Haggerty, R., Hinz, C., Hooper, R., Kirchner, J., Roderick, M.L., Selker, J., Weiler, M., 2007. Moving beyond heterogeneity and process complexity: A new vision for watershed hydrology: OPINION. Water Resour. Res. 43, n/a–n/a. doi:10.1029/2006WR005467

McDonnell, J.J., Woods, R., 2004. On the need for catchment classification. J. Hydrol. 299, 2–3. doi:10.1016/j.jhydrol.2004.09.003

McGlynn, B.L., McDonnel, J.J., Brammer, D.D., 2002. A review of the evolving perceptual model of hillslope flowpaths at the Maimai catchments, New Zealand. J. Hydrol. 257, 1–26. doi:10.1016/S0022-1694(01)00559-5

McGlynn, B.L., McDonnell, J.J., 2003. Role of discrete landscape units in controlling catchment dissolved organic carbon dynamics: CATCHMENT DOC EXPORT. Water Resour. Res. 39, n/a–n/a. doi:10.1029/2002WR001525

McIntyre, N., Lee, H., Wheater, H., Young, A., Wagener, T., 2005. Ensemble predictions of runoff in ungauged catchments. Water Resour. Res. 41, W12434. doi:10.1029/2005WR004289

McNamara, J.P., Tetzlaff, D., Bishop, K., Soulsby, C., Seyfried, M., Peters, N.E., Aulenbach, B.T., Hooper, R., 2011. Storage as a Metric of Catchment Comparison. Hydrol. Process. 25, 3364–3371. doi:10.1002/hyp.8113

Morris, P.J., Waddington, J.M., Benscoter, B.W., Turetsky, M.R., 2011. Conceptual frameworks in peatland ecohydrology: looking beyond the two-layered (acrotelm–catotelm) model. Ecohydrology 4, 1–11. doi:10.1002/eco.191

Nash, Je., Sutcliffe, J.V., 1970. River flow forecasting through conceptual models part I—A discussion of principles. J. Hydrol. 10, 282–290.

National Wetlands Working Group, Canada Committee on Ecological (Biophysical) Land Classification, Warner, B.G., Rubec, C.D.A., 1997. The Canadian wetland classification system. Wetlands Research Branch, University of Waterloo, Waterloo, Ont.

Neiland, B.J., 1971. The forest-bog complex of southeast Alaska. Vegetatio 22, 1–64. doi:10.1007/BF01955719

Nowacki, G., Shepard, M., Krosse, P., Pawuk, W., Fisher, G., Baichtal, J., Brew, D., Kissinger, E., Brock, T., 2001. Ecological subsections of southeast Alaska and neighboring areas of Canada. (No. R10-TP-75). US Department of Agriculture Forest Service, Anchorage, AK.

Oudin, L., Andréassian, V., Perrin, C., Michel, C., Le Moine, N., 2008. Spatial proximity, physical similarity, regression and ungaged catchments: A comparison of regionalization approaches based on 913 French catchments. Water Resour. Res. 44, W03413. doi:10.1029/2007WR006240

Oudin, L., Kay, A., Andréassian, V., Perrin, C., 2010. Are seemingly physically similar catchments truly hydrologically similar? Water Resour. Res. 46, W11558. doi:10.1029/2009WR008887

Pinheiro, J., Bates, D., DebRoy, S., Sarkar, D. and R Core Team (2014). nlme: Linear and Nonlinear Mixed Effects Models. R package version 3.1-117, URL http://CRAN.R-project.org/package=nlme

Poff, N.L., Olden, J.D., Pepin, D.M., Bledsoe, B.P., 2006. Placing global stream flow variability in geographic and geomorphic contexts. River Res. Appl. 22, 149–166. doi:10.1002/rra.902

Post, D.A., Jones, J.A., 2001. Hydrologic regimes of forested, mountainous, headwater basins in New Hampshire, North Carolina, Oregon, and Puerto Rico. Adv. Water Resour., Nonlinear Propagation of Multi-scale Dynamics Through Hydrologic Subsystems 24, 1195–1210. doi:10.1016/S0309-1708(01)00036-7

Price, J.S., 1992. Blanket bog in Newfoundland. Part 2. Hydrological processes. J. Hydrol. 135, 103–119. doi:10.1016/0022-1694(92)90083-8

R Core Team (2014). R: A language and environment for statistical computing. R Foundation for Statistical Computing, Vienna, Austria. URL http://www.R-project.org/.

Rupp, D.E., Selker, J.S., 2006. Information, artifacts, and noise in dQ/dt−Q recession analysis. Adv. Water Resour. 29, 154–160. doi:10.1016/j.advwatres.2005.03.019

Samaniego, L., Bárdossy, A., Kumar, R., 2010. Streamflow prediction in ungauged catchments using copula-based dissimilarity measures. Water Resour. Res. 46, W02506. doi:10.1029/2008WR007695

Sawicz, K., Wagener, T., Sivapalan, M., Troch, P.A., Carrillo, G., 2011. Catchment classification: empirical analysis of hydrologic similarity based on catchment function in the eastern USA. Hydrol. Earth Syst. Sci. 15, 2895–2911. doi:10.5194/hess-15-2895-2011

Sayama, T., McDonnell, J.J., Dhakal, A., Sullivan, K., 2011. How much water can a watershed store? Hydrol. Process. 25, 3899–3908. doi:10.1002/hyp.8288

Schiff, S.L., Aravena, R., Trumbore, S.E., Hinton, M.J., Elgood, R., Dillon, P.J., 1997. Export of DOC from forested catchments on the Precambrian Shield of Central Ontario: clues from 13C and 14C. Biogeochemistry 36, 43–65.

Siegela, D. i., 1988. The Recharge-Discharge Function of Wetlands Near Juneau, Alaska: Part I. Hydrogeological Investigations. Ground Water 26, 427–434. doi:10.1111/j.1745-6584.1988.tb00408.x

Sivapalan, M., 2003. Prediction in ungauged basins: a grand challenge for theoretical hydrology. Hydrol. Process. 17, 3163–3170. doi:10.1002/hyp.5155
Sivapalan, M., 2006. Pattern, Process and Function: Elements of a Unified Theory of Hydrology at the Catchment Scale, in: Encyclopedia of Hydrological Sciences. John Wiley & Sons, Ltd.
Soetaert, K., Petzoldt, R., Setzer, W. (2010). Solving Differential Equations in R: Package deSolve. Journal of Statistical Software, 33(9), 1-25. URL http://www.jstatsoft.org/v33/i90/.
Soil Survey Division Staff, 1993. Soil survey manual, Rev. ed. ed, United States Department of Agriculture handbook. U.S. Dept. of Agriculture, Washington, D.C.
Spence, C., 2007. On the relation between dynamic storage and runoff: A discussion on thresholds, efficiency, and function. Water Resour. Res. 43, n/a–n/a. doi:10.1029/2006WR005645
Spence, C., 2010. A Paradigm Shift in Hydrology: Storage Thresholds Across Scales Influence Catchment Runoff Generation. Geogr. Compass 4, 819–833.
Spence, C., Guan, X.J., Phillips, R., Hedstrom, N., Granger, R., Reid, B., 2009. Storage dynamics and streamflow in a catchment with a variable contributing area. Hydrol. Process. 24, 2209–2221. doi:10.1002/hyp.7492
Spence, C., Guan, X.J., Phillips, R., Hedstrom, N., Granger, R., Reid, B., 2010. Storage dynamics and streamflow in a catchment with a variable contributing area. Hydrol. Process. 24, 2209–2221. doi:10.1002/hyp.7492
Swanson, F.J., Jones, J.A., 2002. Geomorphology and hydrology of the HJ Andrews experimental forest, Blue River, Oregon. Field Guide Geol. Process. Cascadia 289–314.
Taylor, C.H., Pierson, D.C., 1985. The effect of a small wetland on runoff response during spring snowmelt. Atmosphere-Ocean 23, 137–154. doi:10.1080/07055900.1985.9649219
TCW Economics, 2010. Economic Contributions and Impacts of Salmonid Resources in Southeast Alaska. Sacramento, CA.
Teuling, A.J., Lehner, I., Kirchner, J.W., Seneviratne, S.I., 2010. Catchments as simple dynamical systems: Experience from a Swiss prealpine catchment. Water Resour. Res. 46, n/a–n/a. doi:10.1029/2009WR008777
Troch, P.A., Carrillo, G.A., Heidbüchel, I., Rajagopal, S., Switanek, M., Volkmann, T.H.M., Yaeger, M., 2009. Dealing with Landscape Heterogeneity in Watershed Hydrology: A Review of Recent Progress toward New Hydrological Theory. Geogr. Compass 3, 375–392. doi:10.1111/j.1749-8198.2008.00186.x
Tromp-van Meerveld, H.J., McDonnell, J.J., 2006. Threshold relations in subsurface stormflow: 2. The fill and spill hypothesis: THRESHOLD FLOW RELATIONS, 2. Water Resour. Res. 42, n/a–n/a. doi:10.1029/2004WR003800
Waddington, J.M., Roulet, N.T., Hill, A.R., 1993. Runoff mechanisms in a forested groundwater discharge wetland. J. Hydrol. 147, 37–60.
Wagener, T., Sivapalan, M., Troch, P., Woods, R., 2007. Catchment Classification and Hydrologic Similarity. Geogr. Compass 1, 901–931. doi:10.1111/j.1749-8198.2007.00039.x
Wagener, T., Sivapalan, M., Troch, P.A., McGlynn, B.L., Harman, C.J., Gupta, H.V., Kumar, P., Rao, P.S.C., Basu, N.B., Wilson, J.S., 2010. The future of hydrology: An evolving science for a changing world. Water Resour. Res. 46, W05301. doi:10.1029/2009WR008906
Worrall, F., Burt, T.P., Jaeban, R.Y., Warburton, J., Shedden, R., 2002. Release of dissolved organic carbon from upland peat. Hydrol. Process. 16, 3487–3504. doi:10.1002/hyp.1111
Worrall, F., Gibson, H.S., Burt, T.P., 2008. Production vs. solubility in controlling runoff of DOC from peat soils – The use of an event analysis. J. Hydrol. 358, 84–95. doi:10.1016/j.jhydrol.2008.05.037
Zhang, Z., Fukushima, T., Onda, Y., Gomi, T., Fukuyama, T., Sidle, R., Kosugi, K., Matsushige, K., 2007. Nutrient runoff from forested watersheds in central Japan during typhoon storms: implications for understanding runoff mechanisms during storm events. Hydrol. Process. 21, 1167–1178. doi:10.1002/hyp.6677

APPENDIX

Source code and instructions for dynamical modeling in R.

Data Requirements

Application of this method requires a time series of precipitation and discharge and, if you want to use the PET filter and/or simulate a hydrograph, potential evapotranspiration. To simulate a hydrograph, the PET and precipitation time series must be complete (no missing values). Generally, a minimum of several years of data is required, as <10% of the available data will end up being used. Discharge, precipitation, and PET must all have units of depth and all units must be the same. As written, this method will work on daily, hourly, and 15 minute time steps. Additional time steps can easily be added but will require some recoding.

Dependencies

package EcoHydRology

package deSolve

Modeling Steps Cheat Sheet

1) Prepare data

You'll need a time series of streamflow, precipitation and, if you want to simulate a hydrograph, potential evapotranspiration. This series should be as long as possible, as only a small subset will be usable for creating the model. For the R code to work the columns need to be named "time", "q", "pcp", and "pet" for the date/times, discharge, precip, and PET respectively. Discharge, precip, and PET all need to have the same units (depth).

2) Filter data

Use the dm.filter function to create a dataframe of data points where the change in storage is dominated by discharge. Because you probably have PET data you can use the pet filter option. Suggested function arguments are:

pet = T *use the q > 10*precip & pet filter*

night = F *not the nighttime filter*

verbose = F *only output data points that meet the criteria*

preceding = 0 (for daily)

preceding = 3 (for hourly) *If daily data, it doesn't make sense to apply the filter to previous days. If using hourly applying it to several hours preceding can help correct for differences in precip timing between the gauge and all parts of the watershed.*

3) Get Q and dQ values

Use the get.qdq function to calculate dQ and average Q between successive time steps. Use the data frame created by dm.filter for input. Set the timestep argument equal to the timing of your data, either "days", "hours", or "15 mins". Set graph = T to see the resulting values.

4) Bin the data

As described in lecture and the *Kirchner* [2009], you want to split the Q and dQ values into bins and calculate an average Q and dQ for each bin. The binned averages need to capture the overall pattern of the points, so feel free to play with the arguments. In particular, turning the "err" argument on and off and changing the number of bins will affect your results. Suggested starting points are:

bins = 100 *100 bins to start*

err = T *allow the bins to expand if there is too much scatter in each bin*

neg = T *allow the bins to expand if the average –dQ is positive*

graph = T *see how the binning is capturing the general trend*

5) Get the coefficients for the Q / dQ model

Once you have the binned data, you want to fit a curve to them to get the actual sensitivity function. There aren't really any arguments to tweak here.

6) Simulate the hydrograph(!!)

You can use as much of your original dataset as you like. The only requirement is that the data be complete (no skipped time steps). There are a variety of arguments that can affect your results here, especially the integration method, the minimum and maximum discharge values, and the coefficient k. In particular, if your simulation fails and throws an error talking about infinity, the integration was unstable and setting the min and max values can help. Suggested starting points are:

method = "rk4" *This uses a fixed time step Runge-Kutta method that is nice and fast. Alternatively try "ode45" for a more sophisticated and slower integrator.*

min.q *In the case that your integration fails, set this to approximate your minimum observed discharge*

max.q *Setting this equal to approximate your observed max discharge can increase stability and Nash-Sutcliffe values*

k *This is the scaling coefficient for PET, and has the general effect of shifting your whole simulated hydrograph up and down. Physical values are between 0 and 1.*

7) Calculate your Nash-Sutcliffe efficiency.

How'd your do?

Troubleshooting

In case your NS is terrible

Things to try:

1) Do the binned Q / dQ points match the overall distribution? (check output of dm.bin). If not, play with the binning parameters
2) Try different integration methods (e.g. "rk4", "ode45", "euler")
3) Adjust your k, min.q, and max.q values

In case your integration fails

1) Set or adjust your min.q and max.q values

Description of Dynamical Modeling Functions

dm.filtered

Description

Filters the input dataset to select periods where the change in storage is dominated by discharge. Various filters can be applied by optional arguments. Currently support are: filtering for periods when discharge is much larger than precipitation and potential evapotranspiration ("pet") and filtering for nighttime hours when there is no precipitation ("night"). The pet filter can be applied to daily data, the night filter requires higher temporal resolution.

Usage

dm.filter(df, exclude_rising = T, pet = T, night = F, preceding = 0, multiplier = 10, verbose = F, lat = 40)

Arguments

df	Input dataset. Requires columns named "time" for date/time, "q" for discharge, "pcp" for precipitation and, if using the PET filter, "pet" for potential evapotranspiration. Units for q, pcp, and pet must be the same and must match the time step (e.g. millimeters per day)
exclude_rising	If true, deselects periods where the hydrograph is rising for the number of previous time periods specified by the argument "preceding." Outputs the vector "dropping". [TRUE/FALSE]
pet	If true, this applies the pet/pcp filter, which selects periods where discharge is larger than both pcp and pet by the factor specified by the argument "multiplier". Outputs the vector "pet.filter". [TRUE/FALSE]

If the argument "preceding" is set, the filter will also be applied to the number of preceding time periods specified, outputting the vector "pet.dropping". This filter cannot be used with the night filter.

night	If true, this applies the nighttime filter, which uses the PotSolartInst function to select periods where the potential solar insolation is 0 Watts m^{-2} and precipitation is 0. Outputs the vector "night". If the argument "preceding" is set this filter will be applied to the number of preceding time period specified. This filter cannot be used with the pet filter. [TRUE/FALSE]
preceding	Specifies the number of preceding time periods to apply the various filters to. [Int]

multiplier — Factor by which discharge must exceed both precipitation and potential evapotranspiration when using the pet filter. Default value is 10. [Int]

verbose — If true, the function will return all of the logical vectors created by the filters used, allowing debugging and verification. If false, the function will return only record that pass all of the filters applied. If true, be sure to select the correct records when calling the function get.qdq. [TRUE/FALSE].

lat — Latitude of the watershed. This is only required when using the night filter, as it is passed to the function PotSolarInst. Can take values in radians or degrees, values of more than pi/2 and less than –pi/2 will be converted to degrees, so be careful around the equator.

Author

Paul Herendeen

Example

```
filtered <- dm.filter(df = fallcreek, exclude_rising = F, pet = T, night = F, preceding = 3, multiplier = 10,
        verbose = T)
```

dm.getqdq

Description

This calculates the average discharge and change in discharge from the time series provided. Following *Brutsaert and Nieber* [1977] via *Kirchner* [2009], the change in flow between two successive time periods is calculated as $-dQ/dt = (Q_{t-\Delta t} - Q_t) / \Delta t$ and the average discharge over those periods as $(Q_{t-\Delta t} + Q_t) / 2$. It is not necessary that the time series is complete, as the function will create a complete time series with empty values where there are no data. Requires columns to be named "time" and "q". Generally this function is called with the output of dm.filtered

Usage

```
dm.getqdq(df, timestep = NULL, graph = T)
```

Arguments

df — Input dataset. Requires columns to be named "time" and "q". Generally this function is called with the output of dm.filtered

timestep — The timestep of the data. Currently supported are "days", "hours", and "15 mins"

graph — If true this will display a chart of the resulting q and dq values on log axis. [TRUE / FALSE]

Author

Paul Herendeen

Example

qdq <- dm.getqdq(df = filtered[filtered$pet.filter,], timestep = "days")

dm.bin

Description

This bins the calculated q and dq values and calculates an average for each bin, following *Kirchner* [2009]. In general, the function divides the range of the natural log of the discharge values in a fixed number of bins and calculates an average q and dq for each bin. If the various quality filters are set (e.g. "err", "neg"), each bin is further allowed to expand until the filter is satisfied. Requires columns named "qave" and "dq".

Usage

dm.bin(df, err = T, neg = F, bins = 100, graph = T)

Arguments

df	The input dataset. Requires columns to be named "qave" and "dq". Generally this will take the output of the function dm.getqdq
bins	The maximum number of bins, which also sets the minimum width of each bin. If "err" and "neg" are both false this will be that actual number of bins used.
err	If true, each bin is allowed to expand until the standard error of ln(q) in the bin is less than ½ the average of ln(q) in the bin. See *Kirchner* [2009] for details. [TRUE / FALSE]
neg	If true, each bin is allowed to expand until average(ln(-dq)) is positive.
bins	The maximum number of bins. Because the range of ln(qave) is divided by the number of bins this also sets the minimum width of each bin. [Int]
graph	If true, displays a plot of the original qave and dq along with the binned averages on log axes.

Author

Paul Herendeen

Example

binned <- dm.bin(df = qdq, err = T, neg = T, bins = 100, graph = T)

dm.model

Description

This calculates the coefficients for the modeled q / dq relationship:
$g(Q) = \ln\left(\frac{-dQ/dt}{Q}\right) \approx c_1 + c_2 \ln(Q) + c_3(\ln(Q))^2$ See *Kirchner* [2009] for details.

Usage

dm.modeled(df = input)

Arguments

df Input dataframe. Requires columns named "lnqave" and "lndq". Generally this will take the output of dm.binned

Author

Paul Herendeen

Example

modeled <- dm.model(df = binned)

dm.simulate

Description

Uses the calculated sensitivity function *g(Q)* and precipitation and potential evapotranspiration to simulate the hydrograph. At its core this function solves the differential equation
$\frac{dQ}{dt} = \frac{dQ}{dS}\frac{dS}{dt} = g(Q)(pcp - k * pet - Q)$ using a single initial value of Q and supplied values of pcp and pet. See *Kirchner* (2009), section 7 for details.

Usage

dm.simulate(df, start.q = 0.1, method = "ode45", verbose = F, min.q = 0.05, max.q = NULL, k = 0.5, model = NULL, graph = T)

Arguments

df The input dataset, containing a time series of observed discharge, precipitation, and potential evapotranspiration. Requires columns to be named "time", "q", "pcp", and

	"pet", and for the time series to be complete (values of time, pcp, and pet for all evenly spaced time periods between the beginning and end of the time series). Generally this will be the initial dataset used for this whole analysis
start.q	The initial value of discharge. The function will find the first time where discharge equals this value and start the hydrograph simulation there. [numeric]
method	The numerical integration method used to solve the differential equation. This is passed to the function "ode" from the package "deSolve" and needs to be intelligible by that function. Common methods are: "euler", for the basic, fixed-interval Euler method; "rk4" for a classical fixed-timestep, 4th order, Runge-Kutta method, and "ode45" for a variable time-step, Dormand-Prince 4(5), based on the "ode45" function in MATLAB. [character]
verbose	If true, the differential equation function will print a set of diagnostic outputs each time it is called. The printed outputs are the time step, ln(q), q, pcp, pet, and d(ln(q)) where q is the simulated discharge. The differential equation function can be called many times for each time step depending on the integration method used. This is useful for diagnosing integration failures. [TRUE / FALSE]
min.q	Minimum allowable discharge value. If given, this sets a floor for the discharge. This can increase stability of the integration. See *Brauer et al.* [2013] for an example in practice. [Int]
max.q	Maximum allowable discharge value. If given, this sets a ceiling for this discharge. This can increase stability of the integration. [Int]
k	This is a fixed multiplier converting potential evapotranspiration for actual evapotranspiration. In the original conception of this method (*Kirchner* [2009]), this is the only tuneable parameter in the simulation. Default value is 0.3. Physical values are between 0 and 1, although the code can accommodate any value. [Int]
model	A named numeric vector containing the coefficients of the modeled dq / q relationship $\ln\left(\frac{-dQ/dt}{Q}\right) \cong c_1 + c_2 \ln(Q) + c_3(\ln(Q))^2 = g(Q)$. Requires the values to be named "c1", "c2", "c3". Generally this will take the output of dm.model [numeric]
graph	If true, this calls the function "hydrograph" from the EcoHydRology package and displays the observed and modeled discharge and the precipitation.

R Code for dynamical modeling

Author

Paul Herendeen

```
require(EcoHydRology)
require(deSolve)


dm.filter <- function(df, exclude_rising = T, pet = T, night = F, preceding = 0, multiplier = 10, verbose =
F, lat = 40) {
  # check that the necessary columns are included
  if(any(c("time", "q", "pcp") %in% names(df) == F)) {
    stop("dm.filter requires dataframe to have columns named \"time\", \"q\", and \"pcp\"")
  }

  # data quality checks
  if(pet & night) {print("You're trying to use both PET and nightime filtering!!")}

  # night time filtering
  if (night == T) {
    if(attr((df[1,"time"] - df[2,"time"]), "units") == "days") {
      stop("Can't use the night time filter on daily data!!")
    }

    df$night <- PotSolarInst(Jday = (1+as.POSIXlt(df[,"time"])$yday),
                             hour = as.numeric(format(df[,"time"], format = '%H')),
                             lat = lat,
                             SolarNoon= 12) == 0

    if(is.null(preceding)) { preceding <- 1 }

    # deselect records where there was preceding rain
    df$night <- (filter(df[,"pcp"], rep(1, preceding + 1), sides = 1) == 0) & df$night

    # get the first couple records
    df$night[1:preceding] <- F
  }

  # PET filter section
```

```
  if (pet == T) {
    if("pet" %in% names(df) == F) {
      stop("pet filter needs a column named \"pet\"")
    }

    # q is at least 10x pet and p
    df$pet.filter <- (df["q"] > multiplier * df["pcp"]) & (df["q"] > multiplier * df["pet"])
    df$pet.filter[is.na(df$pet.filter)] <- F

    # this applys the filter to the preceding hours, if appropriate
    if(!is.null(preceding)) {
      df$pet.preceding <- as.logical(filter(df$pet.filter, rep(1, preceding + 1), sides=1) == preceding + 1)
      df$pet.preceding[1:(preceding)] <- F
    }
  }

  if(exclude_rising == T) {
    # set up vector showing if q is larger than the preceding
    df$larger <- df["q"] > c(NA, head(df["q"], -1))

    # run length encode the larger vector
    run <- rle(df$larger)

    # if q is only increasing for one time period set the value to F
    run$values[run$values & (run$length < 2)] <- F
    df$rising <- inverse.rle(run)
    #replace NA with FALSE
    df$rising[is.na(df$rising)] <- F
    # invert! this is important
    df$dropping <- !df$rising
    df <- subset(df, select = -c(larger, rising))
  }

  if(verbose == T) {
    return(df)
  } else {
    filters <- as.vector(na.omit(match(c("pet.filter", "night", "dropping", "pet.preceding"), names(df))))
    df <- df[Reduce(`&`, df[, filters, drop = FALSE]), ]
    df <- df[, -filters]
    return(df)
  }
}

dm.getqdq <- function(df, timestep = NULL, graph = T) {
  # check that the necessary columns are included
  if(any(c("time", "q") %in% names(df) == F)) {
    stop("dm.getqdq requires dataframe to have columns named \"time\" and \"q\"")
  }

  if(is.null(timestep)) {
    stop("Need to specify appropriate time step\nacceptable units are 'days' 'hours' '15 mins'")
```

```
  }

  if(!(timestep %in% c("days", "hours", "15 mins"))) {
    stop("Need to specify appropriate time step\nacceptable units are 'days' 'hours' '15 mins'")
  }

  # set up vector of complete time series
  all.times <- data.frame(time = seq(min(df$time), max(df$time), by=timestep))
  df <- merge(all.times, df, by = as.character(names(df)[1]), all.x = T, all.y = F)

  # calculate q and dq
  df$qave <- with(df, (df$q + c(NA, head(df$q, -1)))/2)
  df$dq <- with(df,c(NA, head(df$q, -1)) - df$q)

  if (graph == T) {
    plot(df$qave, df$dq, log="xy", xlab="q", ylab="dq", main="q /\ dq plot",pch=16)
  }

  return(df)
}

dm.bin <- function(df, err = T, neg = F, bins = 100, graph = T) { ####
  # make sure appropriate columns are there
  if(any(c("qave", "dq") %in% names(df) == F)) {
    stop("this function needs a data frame with \"qave\" and \"dq\" as column names!!")
  }

  # cut out NAs
  df <- df[complete.cases(df$qave, df$dq),]
  df <- df[order(df$qave, decreasing=T),]

  #calculate width of bins in log units
  minwidth <- abs((log(0.1)-max(log(df$qave))))/bins
  # set up results dataframe
  results <- matrix(as.numeric(NA), nrow(df),5)

  # initialilze binstart and results pointer
  #bs means bin start
  bs.old <- 1
  bs <- 1
  r <- 1
  n <- nrow(df)

   # run the loop through the dataset
   for(i in 2:n){
     # first check if the bin meets the minimum width and if so calculate the means
     if(abs(log(df$qave[bs])-log(df$qave[i])) >= minwidth) {
       meanq <- mean(df$qave[bs:i])
       meandq <- mean(df$dq[bs:i])
       stderrdq <- (sd(df$dq[bs:i]) / sqrt(length(df$dq[bs:i])))
       # then check if it meets the stderr condition and if so write the results to the table
```

```
      # only do this if error=T and if you're not at the end of the df
      if(((stderrdq > (meandq / 2)) & err==T) | (meandq < 0 & neg == T)) { next }

      results[r,] <- c(bs, i, meanq, meandq, stderrdq)
      r <- r + 1
      bs.old <- i
      bs <- i
     }

   }

  # convert results to data frame
  results <- as.data.frame(results)
  names(results) <- c("start", "end", "qave", "dq", "stderr")
  # add lnq and lndq
  results$lnqave <- log(results$qave)
  results$lndq <- log(results$dq)

  if(graph == T) {
     plot(df$qave, df$dq, log="xy", xlab="qave", ylab="dq", main="q /\ dq plot",pch=16)
     points(results$qave, results$dq, col="blue", pch=16)
    }

  # if bs.old==1 (i.e. no results) return one row of NA, else return the results
   if(bs.old==1) {
     results[r,] <- rep(NA, 5)
     return(results[1,])
   } else {
     return(results[complete.cases(results),])
   }
}

dm.model <- function(df) {
  # check for column names
  if(any(c("lndq", "lnqave") %in% names(df) == F)) {
    stop("dm.filter requires dataframe to have columns named lndq, lnqave")
  }

  temp <- lm(lndq ~ lnqave + I(lnqave^2), df)
  temp <- c(coefficients(temp), summary(temp)$r.squared)
  names(temp) <- c("c1", "c2", "c3", "r^2")

  plot(df$lnqave, df$lndq, xlab="lnqave", ylab="lndq", main="modeled q /\ dq relationship")
  lines(df$lnqave, predict(lm(lndq~lnqave + I(lnqave^2), data=df)),
        col="blue")

  # subtract 1 from c2, to convert ln(dQ/dt) = f(Q) to ln((dQ/dt)/-Q) = g(Q), see Kirchner 2009
  temp['c2'] <- temp['c2'] - 1

  return(temp)
}
```

```
dm.simulate <- function(df, start.q = 0.1, method = "rk4", verbose = F, min.q = 0.05, max.q = NULL, k =
0.5, model = NULL, graph = T) {
  # check that the necessary columns are included
  if(any(c("time", "q", "pcp", "pet") %in% names(df) == F)) {
    stop("dm.filter requires dataframe to have columns named time, q, pcp, and pet")
  }

  # convert min and max stream flow to logs
  if(!is.null(min.q)) {min.lnq <- log(min.q)} else {min.lnq <- -99999}
  if(!is.null(max.q)) {max.lnq <- log(max.q)} else {max.lnq <- 99999}

  # set up the differential equation function
  dlnqdt <- function(t,y,parms) {
    pcp <- df[pmax(1,ceiling(t)), "pcp"]
    pet <- df[pmax(1,ceiling(t)), "pet"]

    dlnq.temp <- exp(c1 + c2 * y + c3 * y ^ 2) * (((pcp - k * pet) / exp(y)) - 1)

    if((y + dlnq.temp) < min.lnq & !is.null(min.lnq)) {
      dlnq <- min.lnq - y
    } else if(y + dlnq.temp > max.lnq & !is.null(max.lnq)) {
      dlnq <- max.lnq - y
    } else {
      dlnq <- dlnq.temp
    }

#
#     if(!is.null(min.q)) {
#       if((y + dlnq.temp) < min.lnq) {
#         dlnq <- min.lnq - y
#       } else { dlnq <- dlnq.temp }
#     } else if(!is.null(max.q)) {
#       if((y + dlnq.temp) > max.lnq) {
#         dlnq <- max.lnq - y
#       } else { dlnq <- dlnq.temp }
#     } else {
#       dlnq <- dlnq.temp
#     }

    if (verbose == T){
      print(c(t,y,exp(y), pcp, pet,dlnq), digits=3, justify="left")
    }

    return(list(dlnq))
  }

  # get the coefficients
  c1 <- model[1]
  c2 <- model[2]
  c3 <- model[3]
```

```
  # find the start time
  start <- min(which(df[2] > start.q))

  # initialize simulated output
  df$qsim <- df$lnqsim <- as.numeric(NA)
  # calculate the first lnqsim
  df$lnqsim[start] <- log(df[start, "q"])

  df$lnqsim[start:nrow(df)] <- as.data.frame(ode(y=df$lnqsim[start],func=dlnqdt,
                                                 times=seq(start,nrow(df),1),
                                                 parms=NULL,method=rkMethod(method)))[,2]

  df$qsim <- exp(df$lnqsim)

  if (graph == T) {
    with(df, hydrograph(streamflow = q, timeSeries=time,
                        streamflow2=qsim, precip=pcp))
  }

  return(df)
}




# get the stream, precip, and pet data
load(file.choose())

# make sure columns are named "time", "q", "pcp", "pet"
names(fallcreek) <- c("time", "q", "pet", "pcp")

# run the filter to select usable data point
filtered <- dm.filter(df=owasco, exclude_rising=F, pet=T, night=F, preceding=NULL, multiplier=10,
verbose=F)

# calculate q and dq
qdq <- dm.getqdq(df=filtered, timestep="days")

# bin the q and dq points
binned <- dm.bin(df=qdq, err=T, neg=T, bins=50, graph=T)

# do the regression to get the model coefficients
modeled <- dm.model(df=binned)

test <- owasco

# run the simulation!
simulated <- dm.simulate(test, start.q=0.1,method="rk4",
                         verbose=F, max.q = 20,
```

```
                k=0.3, model=modeled, graph=T)

# calculate the Nash-Sutcliffe
ns <- NSeff(simulated$q, simulated$qsim)
```